Carbon exchange characteristics and their environmental effects in the northern forest ecosystem of the Greater Khingan Mountains in China

Author

Zhang, Xin, Zhang, Qiuliang, Sun, Shoujia, Xu, Zhihong, Jian, Yanan, Yang, Yue, Tian, Yuan, Sa, Rula, Wang, Bing, Wang, Fei

Published

2022

Journal Title

Science of The Total Environment

Version

Version of Record (VoR)

DOI

10.1016/j.scitotenv.2022.156056

Science of the Total Environment 838 (2022) 156056

Contents lists available at ScienceDirect

Science of the Total Environment

journal homepage: www.elsevier.com/locate/scitotenv

Carbon exchange characteristics and their environmental effects in the northern forest ecosystem of the Greater Khingan Mountains in China

Xin Zhang [a,b], Qiuliang Zhang [a,b,*], Shoujia Sun [c], Zhihong Xu [d], Yanan Jian [a], Yue Yang [e], Yuan Tian [f], Rula Sa [a], Bing Wang [a], Fei Wang [a]

[a] Department of Forest Management, College of Forestry, Inner Mongolia Agricultural University, Hohhot 010019, China
[b] National Field Scientific Observation and Research Station of Greater Khingan Forest Ecosystem, Inner Mongolia, Genhe 022350, China
[c] Research Institute of Forestry, Chinese Academy of Forestry, Beijing 100091, China
[d] Centre for Planetary Health and Food Security, School of Environment and Science, Griffith University, Nathan, Queensland 4111, Australia
[e] Ministry of Education Key Laboratory of Cell Activities and Stress Adaptations, School of Life Sciences, Lanzhou University, Lanzhou 730000, China
[f] College of Life and Environmental Science, Huangshan University, Huangshan 245041, China

HIGHLIGHTS

- CO_2 lake phenomena occur in the forest areas in the northern part of the Greater Khingan Mountains.
- The appearance of a CO_2 lake and its strength responded mainly to temperature changes.
- The CO_2 released during litter decomposition was the main source of CO_2 lake formation.
- The main pathway of C release in the *Larix gmelinii* ecosystem is via autotrophic respiration.

GRAPHICAL ABSTRACT

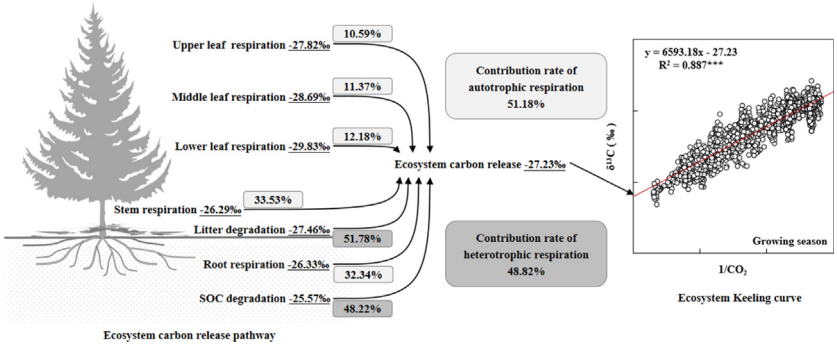

ARTICLE INFO

Editor: Zhaozhong Feng

Keywords:
C exchange
CO_2 concentration
C isotope composition
C release
CO_2 lake phenomenon

ABSTRACT

Measurement and analysis of CO_2 concentration at the ecosystem scale is the basis for studying ecosystem feedback to global climate change, and it is particularly useful for understanding the processes and mechanisms of ecosystem C exchange. Through observation of CO_2 concentration at different heights, this study examined whether a CO_2 lake phenomenon exists in the *Larix gmelinii* ecosystem of the Greater Khingan Mountains (China), and how it might be changed and what might represent its driving factors if such a phenomenon were found to exist. Plants and soils were sampled regularly to determine $\delta^{13}C$ and to quantify the proportion of C released by each component of the ecosystem. The main path of C release and the main source of CO_2 lake formation were investigated. Statistical analysis revealed that a CO_2 lake phenomenon does exist in the *L. gmelinii* ecosystem. Comparative analysis showed that on the daily scale, when the ecosystem was a C source, the CO_2 lake phenomenon often occurred. On the scale of the growing season, the strongest CO_2 lake was accompanied by emergence of the peak respiratory flux. Stepwise regression analysis showed that environmental factors could explain 74.87% of the CO_2 lake phenomenon. The occurrence and strength of the CO_2 lakes were found to mainly respond to changes in temperature. Linear model analysis revealed that the rate of C release from autotrophic respiration in the forest was 51.18%; the rate of C release from heterotrophic respiration during litter decomposition was 51.78%. Therefore, the C release of the *L. gmelinii* ecosystem is mainly from autotrophic respiration. The CO_2 released during decomposition of litter represented the main source for the formation

* Corresponding author at: Department of Forest Management, College of Forestry, Inner Mongolia Agricultural University, Hohhot 010019, China.
E-mail address: 18686028468@163.com (Q. Zhang).

http://dx.doi.org/10.1016/j.scitotenv.2022.156056
Received 18 March 2022; Received in revised form 13 May 2022; Accepted 15 May 2022
Available online 20 May 2022

of CO_2 lakes. The CO_2 lake effect has substantial impact on the net C flux and plays an important role in the C source/sink effect of the ecosystem.

1. Introduction

The global climate change crisis is receiving increasing attention. According to statistics, 2020 was the warmest year since the beginning of the 20th century, and its global average temperature was 1.2 °C higher than that of the preindustrial level (1850–1900) (IPCC, 2021). The continuous increase of atmospheric CO_2 concentration is one of the main causes of global warming (IPCC, 2007). Most countries are attempting to reduce and control their CO_2 emissions, and forests can play an important role in C sequestration (Han et al., 2020; Harris et al., 2021). Establishing and protecting forests is a feasible cost-effective approach to achieving the goal of C neutrality. China is an area that is sensitive to and experiencing notable effects of global climate change, with a rate of temperature increase of 0.26 °C/decade (2011−2020) (CMA Climate Change Centre, 2021). In the Greater Khingan Mountains (China), the rate of temperature increase is 0.4 °C/decade (Zhang et al., 2017), i.e., substantially higher than the national average for the same period. The Greater Khingan Mountains forest area is a key component of the northern forest belt of Eurasia. The cold and humid environment comprising high-latitude permafrost and wetlands (swamps) form China's largest and most concentrated cold-temperate bright coniferous forest area, which represents an important C sink in high-latitude regions (Wang et al., 2020). Those forests, dominated by *Larix gmelinii*, are very sensitive in responding to climate change (Leng et al., 2008). Additionally, in the previous century, large areas of secondary forest formed in the Greater Khingan Mountains forest area because of interference by logging and fire. Currently, only 10% of the original forest in the northern forest area remains undisturbed by humans (data from the Greater Khingan Mountains Forestry Management Bureau). Studying the C exchange process and mechanism of a primary forest ecosystem has important theoretical value and practical significance both for simulating and predicting the role of forest ecosystems in global climate change and for the management of secondary forest ecosystems.

Research on the temporal and spatial dynamics of CO_2 concentration at the forest-ecosystem scale has achieved important results. For example, it has been established that CO_2 concentration varies substantially in different seasons (Forkel et al., 2016), and that the CO_2 concentration at night is higher than that during daytime (Fan et al., 1990). Moreover, the CO_2 concentration at different heights has been shown to exhibit obvious stratification (Broadmeadow et al., 1992). The CO_2 concentration below the canopy decreases with increase in height, and it is higher in the lower canopy than in the upper canopy (Selm, 1952). Many biotic and abiotic factors such as light, water, plant life forms, and forest structure affect the CO_2 concentration of forest ecosystems (Buchmann et al., 1996a, 1997). Different methods such as vorticity correlation (Schaeffer et al., 2008), the box method (Griffith et al., 2012), and the Keeling curve (Keeling, 1958) have been used widely in studies of ecosystem-scale C exchange. However, uncertainty and debate remain regarding the source and the flow of CO_2 during the release process (Atkin et al., 2010; Griffis, 2013). The main reasons are that many biochemical reactions occur during absorption and release of CO_2 (Yakir and Wang, 1996; Wingate et al., 2010), and that CO_2 enrichment occurs over a short period (Chen et al., 2001; Wu et al., 2005). In mountain areas, the atmosphere is generally in a stable state at night, and cold air flows down mountain slopes and gathers in mountain depressions to form cold lakes (Whiteman et al., 2001). Forest ecosystems release more CO_2 at night than during the daytime and the density of the CO_2 is greater than that of the ambient atmosphere. Therefore, it is important to establish whether a CO_2 lake might form under stable atmospheric conditions in forested mountainous terrain, as has been reported in a tropical forest (Zhang et al., 2007). In this study, the phenomenon of a CO_2 lake was defined as a large amount of CO_2 that accumulates in the near-surface atmospheric layer in a valley basin within a certain time range, resulting in sharp increase in its concentration.

The composition of the stable C isotope ($\delta^{13}C$) can be used to track the process of CO_2 exchange in an ecosystem, thereby providing an effective method for distinguishing between photosynthetic C absorption and respiration C release (Ogée et al., 2003; Yakir and Wang, 1996). Photosynthesis increases the heavy isotope of CO_2 in the atmosphere of terrestrial and near-terrestrial ecosystems, while respiration dilutes the heavy isotope of CO_2 in the atmosphere (Buchmann, 2002; Farquhar et al., 1989). The difference between the C isotope fractions can help determine the status of C absorption and C release in an ecosystem during CO_2 exchange (Dawson et al., 2002). The $\delta^{13}C$ dynamics at the ecosystem scale are the combined result of CO_2 exchange, isotope fractionation, and turbulent mixing of air within the boundary layer or the troposphere during photosynthesis and respiration (Lin, 2013; McNaughton et al., 1989). Increasing atmospheric stability enhances the differentiation of $\delta^{13}C$ inside and outside the canopy (Barbour et al., 2011; Flanagan et al., 2012). Ecosystem respiration (Re) is a variable that characterizes the C release of an ecosystem (Davidson et al., 2006), and it can be divided into autotrophic respiration (Ra) and heterotrophic respiration (Rh) according to the respiratory substrate (Grace and Rayment, 2000; Trumbore, 2006). At the canopy scale, the intercept of the Keeling curve usually represents the $\delta^{13}C$ of Re (Dawson et al., 2002). In comparison with the $\delta^{13}C$ of Re, the $\delta^{13}C$ of Ra is depleted, while the $\delta^{13}C$ of Rh is enriched (Flanagan et al., 2005). This difference, which can be used to distinguish between Ra and Rh (Bowling et al., 2002), could thus help in determining the main source of a CO_2 lake. The difference in $\delta^{13}C$ of each component is closely related to plant metabolism and environmental factors (Wingate et al., 2010), and is mainly affected by temperature (Duursma et al., 2014; Fassbinder et al., 2012). Currently, there are no reports on the main sources in CO_2 lake formation or on the driving factors behind CO_2 lake occurrence, making these topics worthy of in-depth study.

In the context of global climate change, permafrost melting, wetland shrinking, and warming and drying trends have exacerbated the functional degradation of the *L. gmelinii* ecosystem (Jiang and Zhou, 2001; Leng et al., 2008; Li et al., 2006). Consensus remains lacking regarding the temporal and spatial dynamics of C exchange, the main pathways of C release, and their driving factors in *L. gmelinii* ecosystems. In this study, we conducted high-frequency observations on the CO_2 concentration and its $\delta^{13}C$ at different heights in the *L. gmelinii* ecosystem of the Greater Khingan Mountains (China), regularly collected different plant organs and different soil components, and detected $\delta^{13}C$ in the samples. Our objectives were to verify whether the CO_2 lake phenomenon occurred in the *L. gmelinii* ecosystem, to reveal the change patterns of any CO_2 lake and its driving factors, to quantify the proportion of C released by each component of the ecosystem, and to determine the main pathways of C release and the main source of CO_2 lake formation. We proposed and verified two hypotheses: (1) that a CO_2 phenomenon exists in the *L. gmelinii* ecosystem, and that its appearance and strength respond mainly to changes in temperature; and (2) that the main pathway of C release in this ecosystem is via Ra, and that Rh is the main source for CO_2 lake formation.

2. Materials and methods

2.1. Study area

The research was undertaken at the National Field Scientific Observation and Research Station (50°49′–50°51′N, 121°30′–121°31′E) of the Greater Khingan Mountains Forest Ecosystem in Inner Mongolia, China from April to October 2020. The station is located in the northwestern part of the Greater Khingan Mountains (Fig. 1), with average elevation of

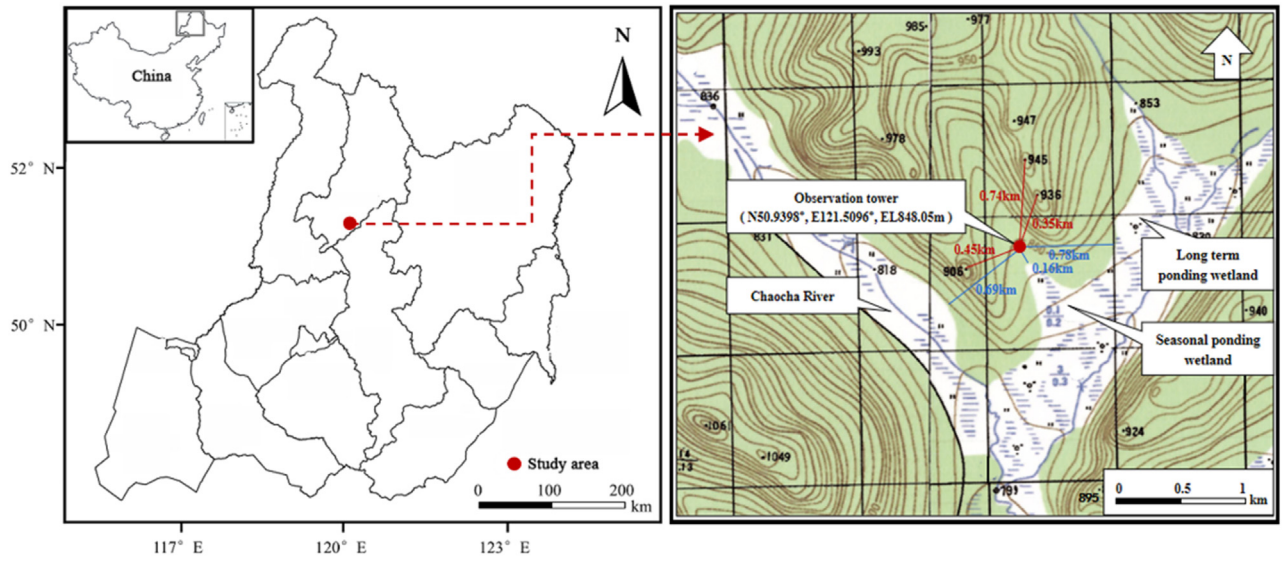

Fig. 1. Location and landform of the study area. The red line represents the straight-line distance between the observation tower and the mountain, and the blue line represents the straight-line distance between the observation tower and the water.

976.5 m. The region is a humid monsoon climate zone within the cold temperate zone. Annual average temperature is −5.4 °C, annual average precipitation is 350–550 mm, the freezing period persists for more than 210 d, and the growing season of vegetation persists for approximately 165 d (Zhang et al., 2021). The soil is mainly brown coniferous forest and swamp soil with thickness of approximately 40–60 cm. Continuous permafrost and island-like frozen soil are staggered within the territory. Frozen soil is an indispensable environmental factor for forest vegetation in this area (Tian et al., 2018). Forests, wetlands, and frozen soils are interdependent and mutually restrictive, forming a unique cold-temperate deciduous coniferous forest landscape.

Both the observation and the sampling areas were located in the comprehensive experimental area of the *L. gmelinii* primary forest in the ecological station. The observation tower was located in an area with gentle undulating slopes in the mountains (Fig. 1). The terrain is relatively low, with average elevation of 848.05 m, surrounded by mountains to the north, rivers to the west, and swampy wetlands to the south and east. Within the area of 1 km^2 around the observation tower, the forest coverage rate was 92%; *L. gmelinii* accounted for more than 90% of the forest, and the remainder was *Betula platyphylla* and *Populus davidiana*. The canopy density was 0.8 and the average tree height was 19.6 m. Understory shrubs included *Rhododendron dauricum*, *Ledum palustre*, *Vaccinium vitis-idaea*, and *Betula fruticosa* with average height of 1.78 m.

2.2. Observation and sampling methods

2.2.1. CO_2 concentration at different heights and its $\delta^{13}C$

Previous studies have shown that the CO_2 flux of *L. gmelinii* ecosystems during the growing season (from late April to early October) followed an obvious single peak variation law, and the daily variation range was −1.09 to 0.11 mg m^{-2} s^{-1}. During the non-growing season (from mid-October to mid-April of the following year), the CO_2 flux was relatively stable, and the daily variation range was less than 0.3 mg m^{-2} s^{-1} (Li and Zhang, 2015; Han et al., 2020). Therefore, during the growing season of the *L. gmelinii* ecosystem, we used a CO_2 stable isotope profile measuring system to analyze the CO_2 concentration and its $\delta^{13}C$ of the ecosystem at six heights: near-surface layer (0.1 m), upper shrub (2 m), lower canopy (10 m), middle canopy (16 m), upper canopy (22 m), and background atmosphere (40 m). The system was based on Off-Axis Integrated Cavity Output Spectroscopy technology, and the $^{13}C/^{12}C$ measurement accuracy was 0.15‰. A CO_2 isotope analyzer (CCIA2, Los Gatos Research Inc., USA) was connected to gas collectors at each vertical level. A polytetrafluoroethylene tube with 1/4-in. outer diameter was used for the connection. A vacuum pump (N940, Los Gatos Research Inc., USA) was used for pumping air and a 16-channel multiplexer (SC-1000, Los Gatos Research Inc., USA) was used to control the gas sampling time at the different heights. The sampling time at each height was 5 min, and a sampling cycle was completed every 30 min. The sampling frequency was 1 Hz and the results output were based on Pee Dee Belemnite (PDB) as the standard, expressed by δ:

$$\delta^{13}C(‰) = \left(\frac{R_{sample}}{R_{s\ tan\ dard}} - 1\right) \times 1000 \quad (1)$$

where R_{sample} and $R_{standard}$ represent the molar ratios of sample and standard $^{13}C/^{12}C$, respectively.

2.2.2. Plant and soil $\delta^{13}C$ measurement

To exclude $\delta^{13}C$ enrichment caused by photosynthesis during daytime, we chose to collect plant and soil samples at night. Choosing a clear night during each phenological period of the growing season, we collected leaves, tree cores, and roots of average-sized *L. gmelinii* within a fixed sample plot (50 × 50 m). Litter and soil samples under the average trees were also collected. Samples with six replicates were placed rapidly into brown sampling bottles after sampling and returned to the laboratory. The samples were dried in an oven at 70 °C for 48 h, crushed through an 80-mesh sieve, and oxidized and reduced to CO_2 at high temperature in a Flash EA1112 HT elemental analyzer (Thermo Fisher Scientific Corp., USA). The stable isotope ratio mass spectrometer (DELTA V ADVANTAGE, Los Gatos Research Inc., USA) was used to detect the $\delta^{13}C$ of CO_2 samples with measurement accuracy of ±0.1‰.

2.2.3. Observation of environmental factors

The observation tower of the CO_2 stable isotope profile measurement system was also equipped with a micrometeorological observation system. The environmental factors of the ecosystem included solar radiation (SR) (CM11, Campbell Scientific, USA), precipitation (P) (52203, RM YOUNG), air temperature (Ta) (HMP45C, VAISALA, Finland), relative humidity (RH) (HMP45C, VAISALA, Finland), wind speed (WS) (CS105, VAISALA, Finland), soil temperature (Ts) (TCVA, Campbell Scientific, USA), and soil moisture content (SWC) (CS616-L50, Campbell Scientific, USA). The sampling frequency of the above measuring instrument was 0.5 Hz. A datalogger (CR1000, Campbell Sci. Inc., USA) automatically

recorded data every 30 min. The saturated vapor pressure difference (VPD) was calculated from Ta and RH (Campbell and Norman, 1998):

$$VPD = a \times \exp\left(\frac{bTa}{Ta + c}\right)(1 - RH) \quad (2)$$

where a, b, c represent constants: 0.611 KPa, 17.50, and 240.97 °C, respectively. The Richardson index (R_i) for evaluating atmospheric stability was calculated from Ta and WS (Mohanal and Siddiquial, 1998):

$$R_i = \frac{g \times \sqrt{c_1 \times c_2}}{T} \times \frac{\theta_1 - \theta_2}{\mu_1 - \mu_1} \times \ln\frac{c_2}{c_1} \quad (3)$$

where g is gravitational acceleration (9.8 m s^{-2}), θ_1 and θ_2 represent potential temperatures (K), and μ_1 and μ_2 represent wind speeds (m s^{-1}) corresponding to heights c_1 and c_2, respectively. Here, T is the average value (K) of the absolute temperature of the two layers of air. A value of $R_i < -0.18$ represents an unstable state; $-0.18 \le R_i < 0.083$ represents a neutral state; and $R_i \ge 0.083$ represents a stable state.

2.3. Data processing

2.3.1. $\delta^{13}C$ of CO_2 released from Re

The Keeling Plot equation was obtained using the reciprocal of the CO_2 concentration and its $\delta^{13}C$ in the ecosystem canopy at the same time, and its intercept was the C isotope composition of CO_2 released from ecosystem respiration ($\delta^{13}C_{Re}$) (Keeling, 1958):

$$\delta^{13}C_a = C_b\left(\delta^{13}C_b - \delta^{13}C_{\mathrm{Re}}\right)\left(\frac{1}{C_a}\right) + \delta^{13}C_{\mathrm{Re}} \quad (4)$$

where C_a and $\delta^{13}C_a$ represent the CO_2 concentration and $\delta^{13}C$ of the atmosphere of the ecosystem, and C_b and $\delta^{13}C_b$ represent the CO_2 concentration and $\delta^{13}C$ of the background atmosphere, respectively.

2.3.2. $\delta^{13}C$ of CO_2 released from Ra

The $\delta^{13}C$ of CO_2 released by canopy leaf respiration is approximately 3‰ higher than that of leaves (Bowling et al., 2008), and the $\delta^{13}C$ of CO_2 released by stem respiration is approximately 1.3‰ higher than that of stems (Klumpp et al., 2005). In the process of CO_2 release from root respiration, C isotope fractionation occurs but the change is small (<1‰) (Moyes et al., 2010). The $\delta^{13}C$ of CO_2 released from autotrophic respiration ($\delta^{13}C_{Ra}$) is the average the $\delta^{13}C$ of CO_2 released by the respiration of plant organs (Chen and Chen, 2007):

$$\delta^{13}C_{Ra} = \overline{\left(\delta^{13}C_{leaf} + 3\right) + \left(\delta^{13}C_{stem} + 1.3\right) + \delta^{13}C_{root}} \quad (5)$$

where $\delta^{13}C_{leaf}$, $\delta^{13}C_{stem}$, and $\delta^{13}C_{root}$ represent the $\delta^{13}C$ values of leaf, stem, and root, respectively.

2.3.3. $\delta^{13}C$ of CO_2 released from Rh

In the process of heterotrophic respiration of soil microorganisms or other organisms, although the change of $\delta^{13}C$ cannot be measured directly, C isotope fractionation does not occur in the process of mitochondrial respiration (Lin and Ehleringer, 1997); therefore, during the decomposition of soil organic matter, $\delta^{13}C$ does not change substantially (Cai et al., 2008). Thus, the average $\delta^{13}C$ of litter and soil organic matter can be used as the $\delta^{13}C$ of CO_2 released during decomposition ($\delta^{13}C_{Rh}$) (Sun et al., 2015):

$$\delta^{13}C_{Rh} = \overline{\delta^{13}C_{litter} + \delta^{13}C_{SOM}} \quad (6)$$

where $\delta^{13}C_{litter}$ and $\delta^{13}C_{SOM}$ represent the isotope components of litter and soil organic matter, respectively.

2.3.4. Quantification

The contribution of autotrophic respiration to ecosystem respiration (F_{Ra}) was calculated using a binary linear mixed model (Yakir and Sternberg, 2000):

$$F_{Ra} = \frac{\delta^{13}C_{\mathrm{Re}} - \delta^{13}C_{Rh}}{\delta^{13}C_{Ra} - \delta^{13}C_{Rh}} \times 100\% \quad (7)$$

The contribution of heterotrophic respiration to ecosystem respiration (F_{Rh}) was determined as follows:

$$F_{Rh} = 1 - F_{Ra} \quad (8)$$

2.3.5. CO_2 concentration and its $\delta^{13}C$ sensitivity to temperature

An exponential regression model was used to fit the relationship between CO_2 concentration and its $\delta^{13}C$ and temperature (Lloyd and Taylor, 1994):

$$CO_2/\delta^{13}C = \alpha e^{\beta T} \quad (9)$$

where T is temperature, α and β are constants. The temperature sensitivity (Q_{10}) of CO_2 concentration and its $\delta^{13}C$ was calculated using the following formula (Boone et al., 1998):

$$Q_{10} = e^{10\beta} \quad (10)$$

2.4. Data analysis

Data were collected using a CO_2 stable isotope profile measurement system that performed circular observations in the order of vertical heights. At the beginning of the observation at each height there would be residual gas from the previous test in the intake pipe. To eliminate the influence of residual gas, the values at the beginning of 0.5, 0.5, 1, 1, 1.5, and 2 min were eliminated for the corresponding heights of 0.1, 2, 10, 16, and 16, 22, and 40 m, respectively. The CO_2 concentration and its $\delta^{13}C$ observation data during different phenological periods in the growing season of the *L. gmelinii* ecosystem were used to study the characteristics of the CO_2 lake. Data analysis was performed using SPSS 26.0 software. The temporal and spatial dynamics of CO_2 concentration and its $\delta^{13}C$ of the ecosystem were analyzed using one-way ANOVA. The significance of CO_2 concentration and its $\delta^{13}C$ difference at different heights was analyzed by independent sample *t*-tests. The relationships between CO_2 concentration, its $\delta^{13}C$, and environmental factors were analyzed by stepwise regression, a linear equation was established, and a significance test was performed. The relationships between CO_2 concentration, its $\delta^{13}C$, and temperature were analyzed by exponential regression, and predicting their trend with global warming.

3. Results

3.1. Phenology and environmental characteristics

During the study period, the growing season of the *L. gmelinii* ecosystem was approximately 165 d (mid-April to early October) (Table 1). The bud opening period (BOP) was approximately 15 d, the leaf opening period (LOP) was approximately 30 d, the leaf spreading period (LSP) was approximately 75 d, and the leaf discoloring period (LDP) combined with the falling period (LFP) was approximately 45 d. The longest phenological period was LSP, which accounted for approximately half of the entire growing season. Leaf area index (LAI) presented a single-peak variation on the growing-season scale with the peak (1.06) at LSP. LSP had the highest rate of C absorption and C release in the *L. gmelinii* ecosystem during the entire growing season. The largest net C absorption of the ecosystem occurred in this period.

Among the environmental factors, Ta and RH both presented a single-peak variation throughout the entire study period (Fig. 2a), reaching their

Table 1
Phenological characteristics of *Larix gmelinii* ecosystem (Mean ± SD).

Phenological period	Time interval	Duration/d	Average occurrence date	LAI	Sunrise time	Sunset time
BOP	Mid-Apr.–late Apr.	15	Apr. 20	0.00	04:00 ± 00:20	19:40 ± 00:10
LOP	Early May–Early Jun.	30	May 5	0.62 ± 0.07	03:45 ± 00:15	19:50 ± 00:15
LSP	Mid-Jun.–Mid-Aug.	75	Jun. 15	1.06 ± 0.13	04:00 ± 00:20	19:40 ± 00:25
LDP	Late Aug.–late Sep.	30	Aug. 25	0.91 ± 0.05	04:20 ± 00:10	19:30 ± 00:20
LFP	Early Sept.–Early Oct.	35	Sept. 5	0.43 ± 0.15	04:30 ± 00:30	19:20 ± 00:30

BOP, LOP, LSP, LDP and LFP represent the bud opening, leaf opening, spreading, discoloring and falling period respectively.

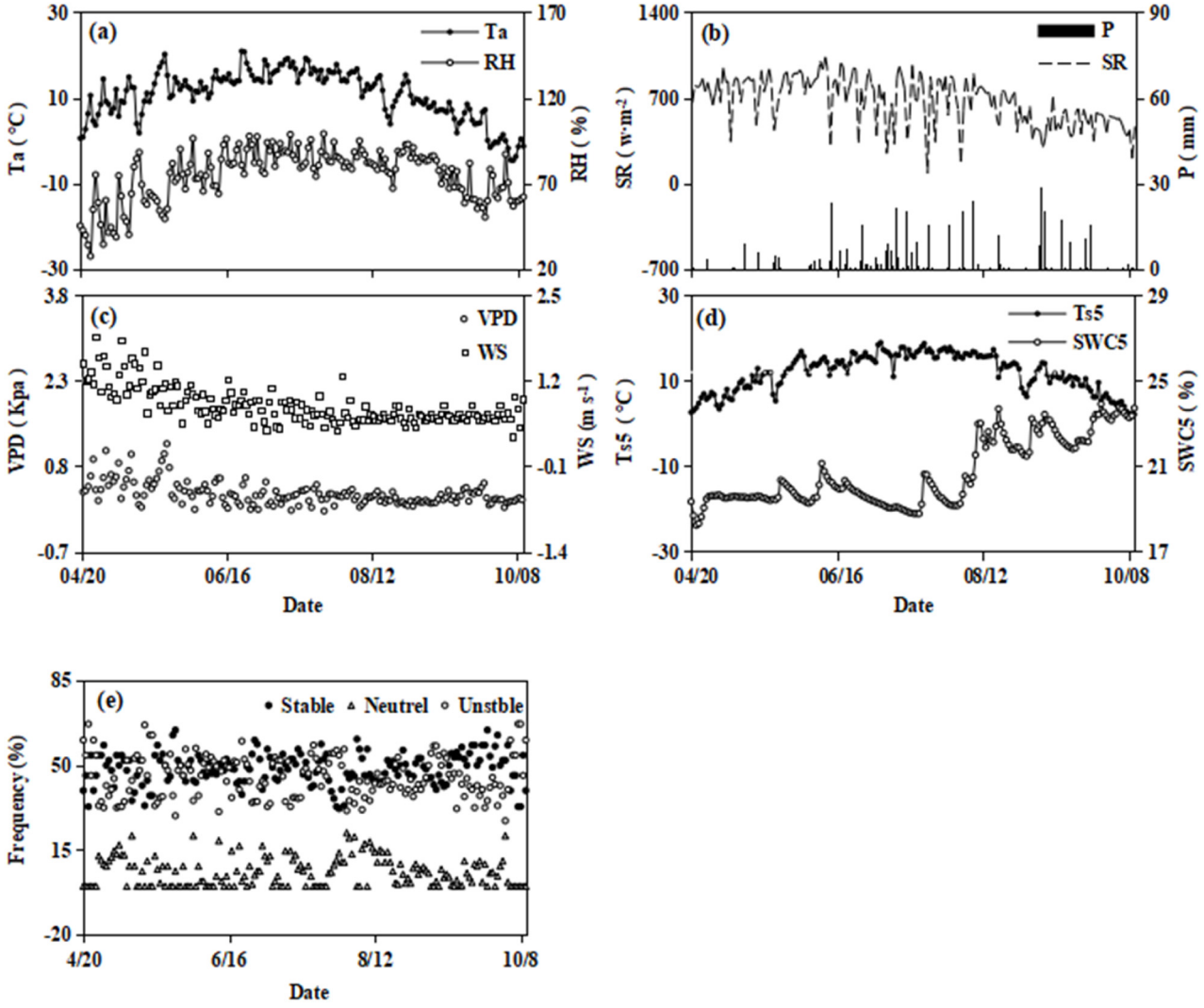

Fig. 2. Variations of air temperature (a), relative humidity (a), solar radiation (b), precipitation (b), water vapor pressure deficit (c), wind speed (c), 5 cm soil temperature (d), 5 cm soil water content (d), and atmospheric stability(e) during the study period.

respective peaks at LSP. At the beginning of the growing season, Ta was notably higher than that at the end, whereas the change of RH showed the opposite pattern of variation to Ta. A single-peak variation was also shown by P (Fig. 2b), i.e., P was small and concentrated at LSP, and reached its peak in the early stage of LDP and LFP with approximately 60% of its annual amount. SR showed decreasing variation (Fig. 2b), and the maximum occurred at LOP. Both VPD and WS also showed decreasing variation (Fig. 2c), but their respective maxima appeared in BOP; their values fluctuated greatly in the early period of the growing season and stabilized in the later period. Affected by Ta, Ts at 5-cm depth (Ts5) also presented a unimodal variation (Fig. 2d), reaching a peak at LSP. The overall fluctuation of Ts5 was smaller than that of Ta. However, SWC5 was affected by both P and Ta, showing increasing variation (Fig. 2d) and reaching its peak in the late growing season. Atmospheric stability did not change substantially during the growing season (Fig. 2e). The distribution frequency of stable and unstable atmospheric states in each phenological period varied between 30% and 70%, and the distribution frequency of neutral atmospheric states varied in a range of 0%–20%.

3.2. CO_2 concentration and its $\delta^{13}C$ changes during the growing season

The daily average value of CO_2 concentration at different heights of the *L. gmelinii* ecosystem presented a single-peak variation at the growing-season scale (Fig. 3a). The daytime average value showed a single-valley variation and the minimum value (379.72 ppm) appeared in LOP (Fig. 3b). However, the nighttime average showed a single-peak variation,

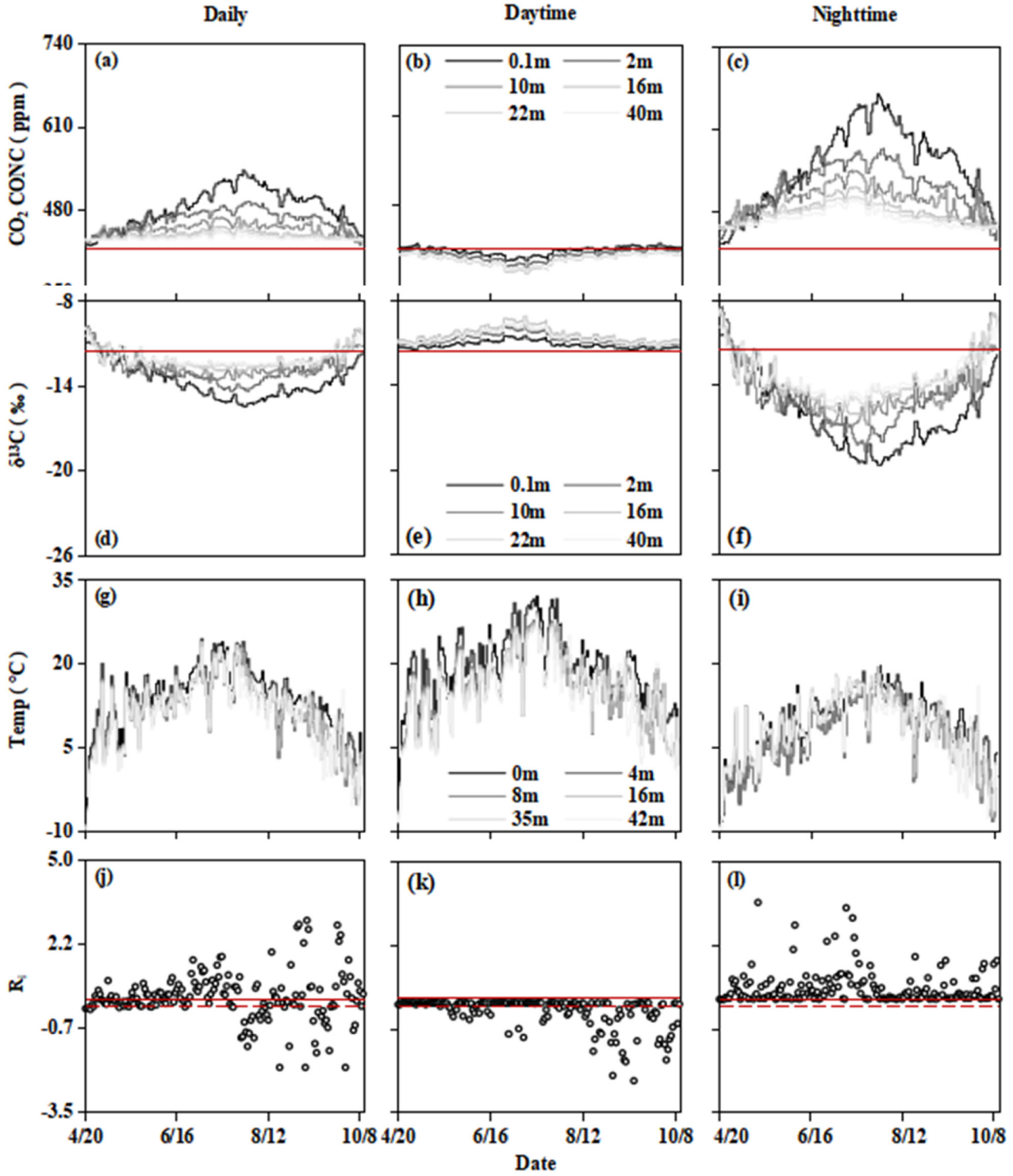

Fig. 3. Variations of CO_2 concentration (a–c), carbon isotopic composition (d–f), air temperature (g–i) and atmospheric stability (j–l) in growing season. In (a–c), the red line represents the CO_2 background concentration of 420 ppm in the observation area. In (d–f), the red line represents the carbon isotopic composition value of −11.5‰ when the CO_2 concentration is 420 ppm. In (j–l), $R_i < -0.18$ is unstable, $-0.18 \leq R_i < 0.083$ is neutral, and $R_i \geq 0.083$ is stable. The red dotted line represents the boundary between instability and neutrality, and the solid line represents the boundary between neutrality and stability.

and the maximum value (664.95 ppm) appeared in LSP (Fig. 3c). The variation of $\delta^{13}C$ change at all heights was the opposite to that of CO_2 concentration (Fig. 3d). The maximum daytime (−9.21‰) (Fig. 3e) and minimum nighttime (−19.74‰) (Fig. 3f) values appeared in LOP and LSP, respectively. The daily average value of Ta at different heights showed a single-peak variation at the growing-season scale, and the maximum value (24.37 °C) appeared in LSP (Fig. 3g). During daytime photosynthesis, the CO_2 concentration decreased with increase of Ta (Fig. 3h). However, during nighttime respiration, the CO_2 concentration increased with increase of Ta (Fig. 3i). The concentrations of CO_2 and its $\delta^{13}C$ at different heights were notably different and there was clear stratification. The stratification was very susceptible to the influence of the state of atmospheric

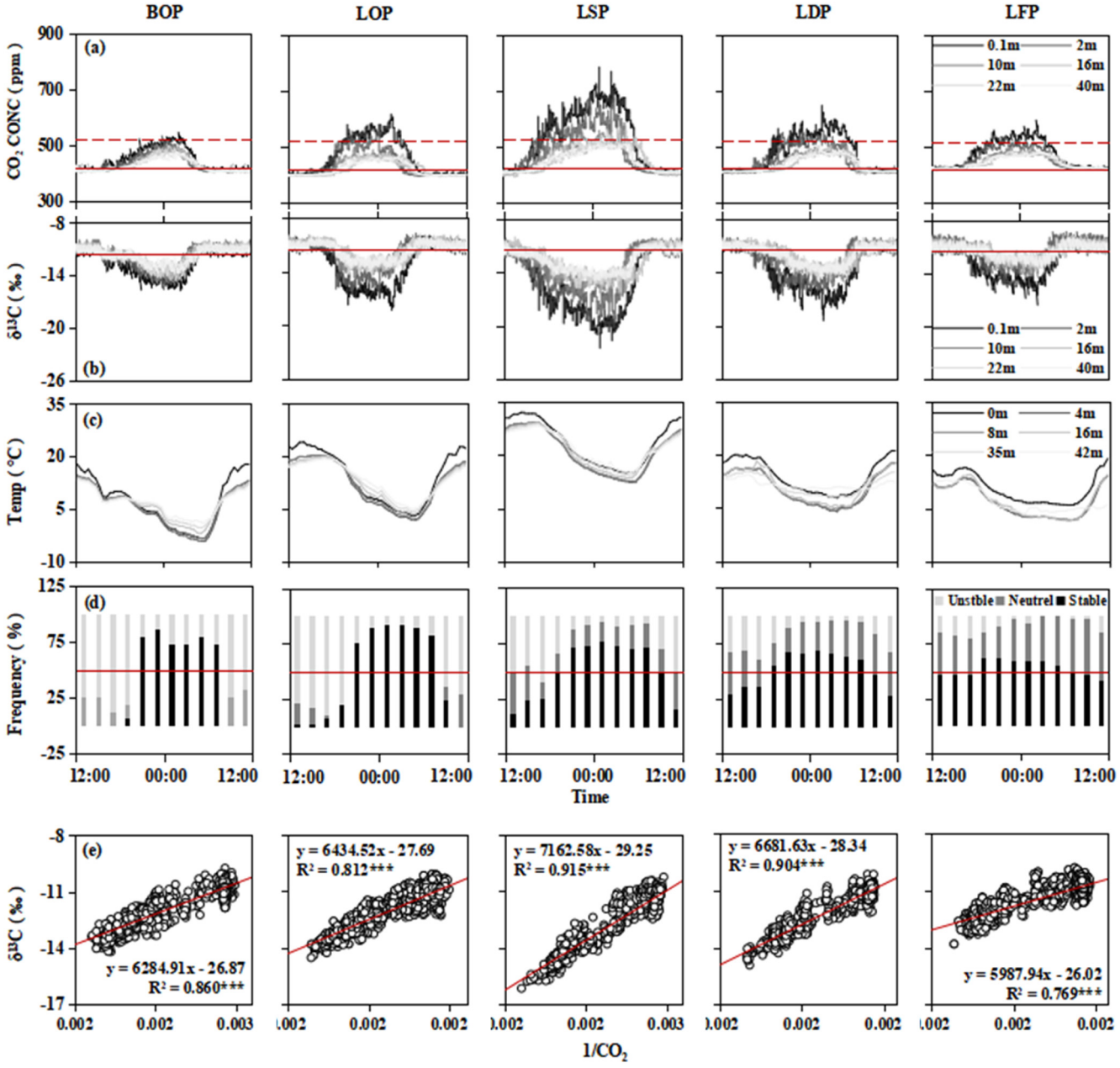

Fig. 4. Variations of CO_2 concentration (a), carbon isotopic composition (b), air temperature (c), atmospheric stability (d) and Keeling curve (e) in different phenological periods. In (a), the red solid line represents the CO_2 background concentration of 420 ppm in the observation area, and the red dotted line represents the reference line 520 ppm when the carbon Lake phenomenon occurs. In (b), the red line represents the carbon isotopic composition value of −11.5‰ when the CO_2 concentration is 420 ppm. In (d), the red line represents that the frequency of atmospheric stability is 50%. In (e), the red line represents Keeling Plot equation, and its intercept represents the carbon isotopic composition value of CO_2 released by the ecosystem. *** means $P < 0.001$, ** means $P < 0.01$, and * means $P < 0.05$.

stability (Fig. 3j). During the day, the atmosphere was mostly in an unstable state (Fig. 3k), and the CO_2 concentration below the canopy decreased with increase of vertical height. The CO_2 concentration above the canopy was notably higher than that within the canopy but lower than that below the canopy. At night, the atmosphere was mostly in a stable state (Fig. 3l), and with increase of vertical height, the CO_2 concentration showed decreasing variation but $\delta^{13}C$ showed increasing variation.

3.3. CO_2 concentration and its $\delta^{13}C$ changes in different phenological periods

The change of CO_2 concentration was found correlated with LAI. The physiological activity of the vegetation was most vigorous and the CO_2 exchange was most obvious during the period of largest LAI. The CO_2 concentration during each phenological period was higher in the near-surface layer and lower in the canopy and above (Fig. 4a). The CO_2 concentration in the surface layer showed a single-peak variation on the daily scale, with a peak at approximately 02:00 in the morning. The largest peak (782.81 ppm) and the smallest peak (547.12 ppm) appeared in LSP and BOP, respectively; the lowest value (406.07 ± 10.79 ppm) appeared at around 11:00. The CO_2 concentration in the canopy and above also showed a single-peak variation on the daily scale, with a peak at approximately 02:00 in the morning (526.78 ± 33.88 ppm), and the lowest value at around 11:00 (402.12 ± 10.22 ppm).

The daily difference (the maximum minus the minimum) of CO_2 concentration near the surface layer (0.1 m) in each phenological period was ≥100 ppm, and a large amount of accumulation occurred during

22:00–02:00 (Fig. 4a), indicating that a CO2 lake phenomenon occurred in the study area. A CO_2 lake appeared in all phenological periods, and CO_2 lake intensity was correlated positively with LAI, with both peaking in LSP (782.81 ppm). From the perspective of the entire growing season, CO_2 lake intensity was stronger in the early morning (00:00–06:00; 578.65 ppm) than in the evening (18:00–00:00; 549.86 ppm), the intensity at night (18:00–06:00 next day; 564.25 ppm) was greater than that during daytime (06:00–18:00; 525.59 ppm), and the intensity in the rainy season (July–August; 562.04 ppm) was greater than that in the less rainy season (May–June; 547.01 ppm).

The changes of $\delta^{13}C$ at different heights in each phenological period showed a single-valley variation (Fig. 4b). Daytime photosynthesis enriched the ^{13}C of CO_2 in the near-surface atmosphere. The maximum value of $\delta^{13}C$ (−9.94‰) appeared in LOP. During this period, SR was strongest and the most photosynthetic C was absorbed in the canopy. Nocturnal respiration depleted the ^{13}C of the CO_2 in the near-surface atmosphere. The minimum value of $\delta^{13}C$ (−22.48‰) appeared in LSP. During this period, Ta was highest and the respiratory C release of the vegetation was largest. Changes in $\delta^{13}C$ released by ecosystem C also showed a single-valley variation (Fig. 4e), with the maximum value (−26.02‰) and minimum value (−29.25‰) appearing in LFP and LSP, respectively.

The changes of Ta at different heights in each phenological period showed a single-valley variation (Fig. 4c). The minimum value (4.98 ± 5.40 °C) appeared during 02:00–04:00, and the maximum value (19.46 ± 5.87 °C) appeared during 12:00–14:00. The Ta at each height during the day was notably different, decreasing with increase of vertical height. At night, the difference in Ta between each height was small and the variation was broadly consistent. On the daily scale, the variation of CO_2 concentration was the opposite to that of Ta. At noon, Ta was highest and photosynthetic C absorption was strongest, resulting in the lowest CO_2 concentration of the day. Affected by the temperature inversion layer at night, the CO_2 released by respiration accumulated in the forest, and reached its peak diurnal value before sunrise owing to the cumulative effect. After sunrise, the flux "flushing" phenomenon occurred and the CO_2 concentration decreased rapidly.

Increase in atmospheric stability increased the difference both in the CO_2 concentration between inside and outside the canopy and in its $\delta^{13}C$ (Fig. 4d). Starting at 06:00, the frequency of occurrence of atmospheric instability increased, reaching a peak at approximately 16:00 (92.31%), following which it began to decline. Starting from 18:00, the frequency of occurrence of the stable state of the atmosphere increased. Contrary to the unstable variation, it reached a peak at approximately 00:00 (95.12%), following which it began to decline, based on a lower state at 10:00–18:00. The time of occurrence of the peak of the CO_2 concentration and the valley of the $\delta^{13}C$ was broadly the same as the time at which the atmosphere appeared extremely stable, except for a small lag effect between the two.

3.4. Drivers of a CO_2 lake

Stepwise regression analysis between CO_2 concentration and its $\delta^{13}C$ at different heights and environmental factors (SR, P, Ta, RH, VPD, WS, Ts5, and SWC5) in the growing season showed that environmental factors could explain 74.87% of the changes of CO_2 concentration and its $\delta^{13}C$. The near-surface CO_2 concentration and its $\delta^{13}C$ change were controlled mainly by Ts5 (Table 2). The CO_2 concentration was correlated positively with Ts5 ($P < 0.001$), whereas $\delta^{13}C$ was correlated negatively with Ts5 ($P < 0.001$). The changes of CO_2 concentration and its $\delta^{13}C$ at the height of the shrub layer and above were driven mainly by Ta, which showed positive correlation with CO_2 concentration ($P < 0.001$) but negative correlation with $\delta^{13}C$ ($P < 0.001$). Overall, the appearance and strength of the CO_2 lake phenomenon in the *L. gmelinii* ecosystem responded mainly to changes in temperature.

3.5. CO_2 concentration below the canopy and its $\delta^{13}C$ change

The change in CO_2 concentration occurred mainly below the canopy, and the change in CO_2 concentration at and above the canopy was small (Fig. 5a). The difference in CO_2 concentration below the canopy (ΔCO_2) was greater in the early morning than in the evening, greater at night than during the day, and greater in the rainy season than in the less rainy season. The magnitude of the difference was correlated positively with the appearance of the CO_2 lake. The largest difference (175.93 ± 96.47 ppm) in CO_2 concentration below the canopy in each phenological phase appeared at approximately 02:00, and the smallest difference (−14.92 ± 15.24 ppm) occurred at approximately 11:00. The biggest difference (272.39 ppm) in the rainy season occurred in LSP, and the smallest difference (74.36 ppm) in the less rainy season occurred in LOP. The variation of the $\delta^{13}C$ difference ($\Delta\delta^{13}C$) below the canopy was the opposite to that of ΔCO_2 (Fig. 5b), but the time of occurrence of both the largest difference (7.67‰) and the smallest difference (0.01‰) was consistent with that of ΔCO_2.

3.6. Influence of environmental factors on the CO_2 concentration and its $\delta^{13}C$ below the canopy

During daytime, ΔCO_2 was correlated positively with both Ta ($P < 0.01$) and RH ($P < 0.05$) but correlated negatively with WS ($P < 0.05$) (Fig. 6a). The increase of Ta and RH during the day was conducive to photosynthetic C absorption in the canopy, causing the CO_2 concentration of the canopy to

Table 2
Stepwise regression analysis of CO_2, $\delta^{13}C$ and environmental factors in *Larix gmelinii* ecosystem.

Item	Height/m	Stepwise regression equation	Coefficient R^2	Significance P	Number n
CO_2	0.1 m	$CO_{2\text{-}0.1m} = 4.244\ Ts_5^{***} - 34.219 WS^{***} - 0.025\ SR^{***} + 0.031\ RH^{**} + 454.815$	0.790	<0.001	8352
	2 m	$CO_{2\text{-}2m} = 0.553\ Ta^{***} - 12.502\ WS^{***} + 0.246\ RH^{***} + 1.889\ Ts_5^{***} + 425.196$	0.834	<0.001	8352
	10 m	$CO_{2\text{-}10m} = 0.490\ Ta^{***} - 5.193\ WS^{***} + 0.665\ Ts_5^{**} + 0.105\ RH^{*} + 433.593$	0.612	<0.001	8352
	16 m	$CO_{2\text{-}16m} = 0.602\ Ta^{***} - 5.980\ WS^{***} - 1.244\ SWC_5^{***} + 0.058\ RH^{*} + 459.716$	0.705	<0.001	8352
	22 m	$CO_{2\text{-}22m} = 0.346\ Ta^{***} - 4.877\ WS^{***} - 0.561\ SWC_5^{***} + 0.042\ RH^{**} + 0.134\ Ts_5^{*} + 443.695$	0.733	<0.001	8352
	40 m	$CO_{2\text{-}44m} = 0.857\ Ta^{***} - 3.640\ WS^{***} + 0.172\ Ts_5^{***} + 0.040\ RH^{*} + 450.542$	0.818	<0.001	8352
$\delta^{13}C$	0.1 m	$\delta^{13}C_{0.1m} = -0.145\ Ts_5^{***} + 1.254\ WS^{***} - 0.144\ SWC_5^{***} - 0.013\ RH^{***} + 0.001\ SR^{**} - 0.038\ Ta^{*} - 9.158$	0.836	<0.001	8352
	2 m	$\delta^{13}C_{2m} = -0.069\ Ta^{***} - 0.017\ Ts_5^{***} + 0.734\ WS^{***} - 0.009\ RH^{*} - 10.275$	0.782	<0.001	8352
	10 m	$\delta^{13}C_{10m} = -0.051\ Ta^{***} - 0.071\ Ts_5^{***} - 0.013\ RH^{***} - 0.122\ SWC_5^{***} + 0.304\ WS^{*} - 8.015$	0.730	<0.001	8352
	16 m	$\delta^{13}C_{16m} = -0.043\ Ta^{***} - 0.062\ Ts_5^{***} + 0.337\ WS^{**} - 0.007\ RH^{*} - 10.715$	0.708	<0.001	8352
	22 m	$\delta^{13}C_{22m} = -0.068\ Ta^{***} - 0.061\ Ts_5^{***} - 0.099\ SWC_5^{***} - 0.006\ RH^{*} - 8.144$	0.809	<0.001	8352
	40 m	$\delta^{13}C_{44m} = -0.048\ Ta^{***} - 0.090\ SWC_5^{***} - 0.040\ Ts_5^{***} - 0.006\ RH^{*} - 8.847$	0.726	<0.001	8352

$CO_{2\text{-}0.1m}$, $CO_{2\text{-}2m}$, $CO_{2\text{-}10m}$, $CO_{2\text{-}16m}$, $CO_{2\text{-}22m}$ and $CO_{2\text{-}44m}$ represent the CO_2 concentration of 0.1, 2,10, 16, 22 and 40 m respectively. $\delta^{13}C_{0.1m}$, $\delta^{13}C_m$, $\delta^{13}C_{10m}$, $\delta^{13}C_{16m}$, $\delta^{13}C_{22m}$ and $\delta^{13}C_{44m}$ represent the $\delta^{13}C$ of 0.1, 2,10, 16, 22 and 40 m respectively.

*** Means $P < 0.001$.

** Means $P < 0.01$.

* Means $P < 0.05$.

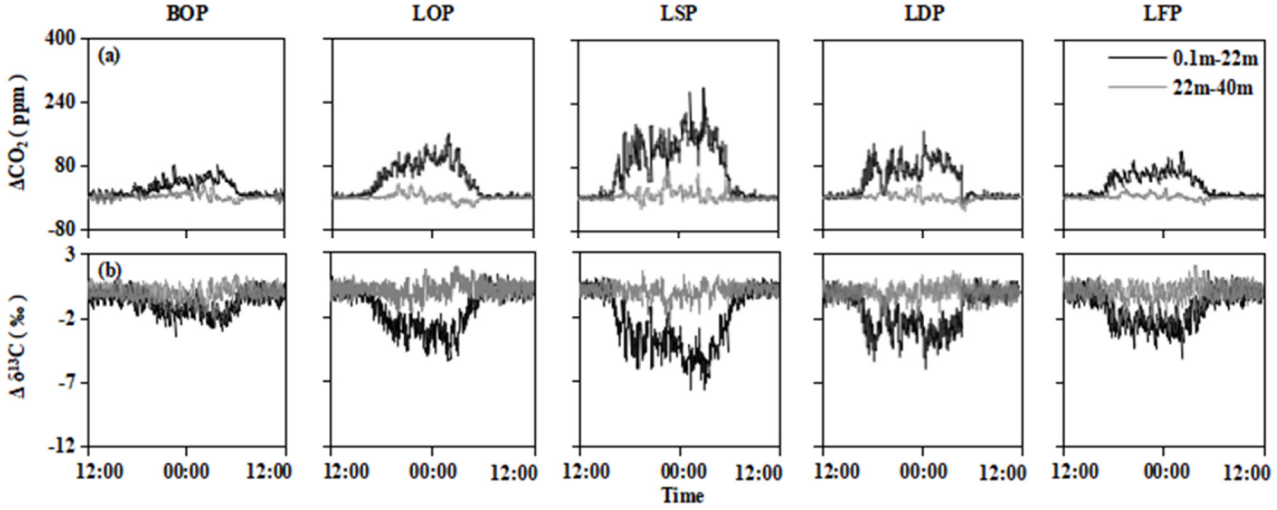

Fig. 5. Differences of CO_2 concentration(a) and $\delta^{13}C$(b) value between the near-ground-surface layer (0.1 m) and upper canopy (22 m), upper canopy and atmosphere (40 m) of *Larix gmelinii* ecosystem.

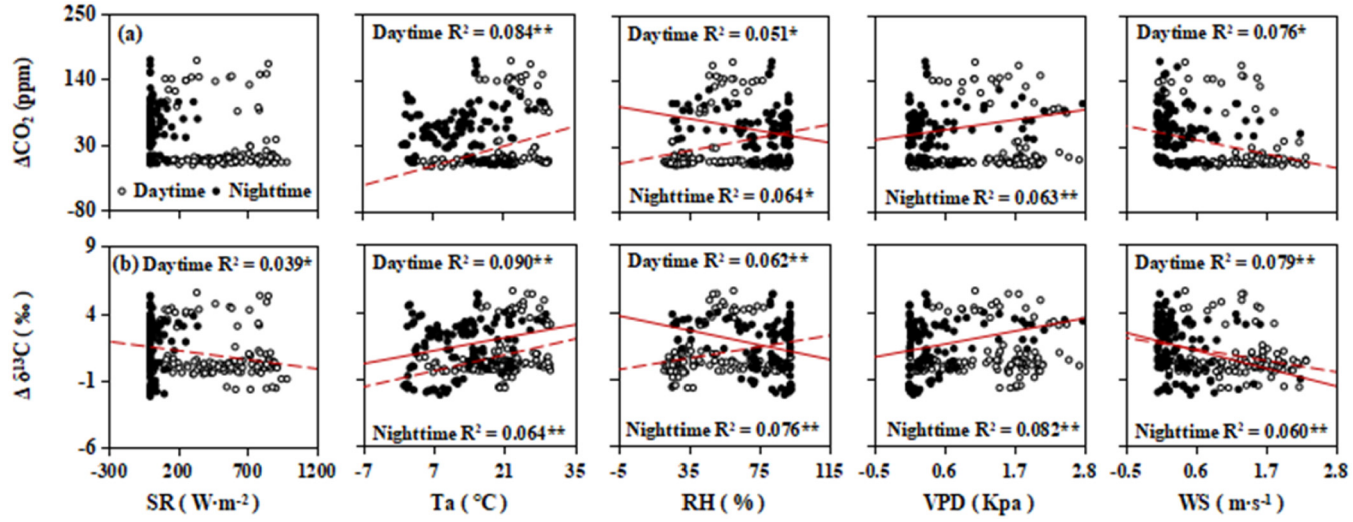

Fig. 6. Linear regression analysis of ΔCO_2, $\Delta\ \delta^{13}C$ and environmental factors in *Larix gmelinii* ecosystem. In (a) and (b), the red dotted line and solid line represent the linear regression of day and night, respectively. *** means $P < 0.001$, ** means $P < 0.01$, and * means $P < 0.05$.

be notably lower than that of the surface layer, and increasing the variation in CO_2 concentration between the different heights. Increase of WS during the day was conducive to the diffusion of CO_2, which reduced the difference in CO_2 concentration between different heights. At night, ΔCO_2 was correlated negatively with RH ($P < 0.05$) and correlated positively with VPD ($P < 0.01$) (Fig. 6a). When RH at night was high, Ta decreased, thereby reducing the activity of respiratory enzymes and resulting in a decrease in the CO_2 concentration difference between the different heights in the forest.

During the day, $\Delta\delta^{13}C$ was correlated negatively with both SR ($P < 0.05$) and WS ($P < 0.01$), and correlated positively with both Ta ($P < 0.01$) and RH ($P < 0.01$) (Fig. 6b). When SR increased during the day, it was beneficial to photosynthetic C absorption by the canopy leaves, which enriched the ^{13}C of CO_2 in the atmosphere such that the $\delta^{13}C$ difference between the various heights was reduced. When WS increased, CO_2 was rapidly diffused, which also caused a difference in $\delta^{13}C$ between the various heights, i.e., the $\delta^{13}C$ difference was reduced accordingly. At night, $\Delta\delta^{13}C$ was correlated positively with both Ta ($P < 0.01$) and VPD ($P < 0.01$) and correlated negatively with both RH ($P < 0.01$) and WS ($P < 0.01$) (Fig. 6b). When Ta increased at night, it increased the activity of respiratory enzymes and promoted the release of respiratory C. Different values of Ta at different heights can affect C release to varying degrees, increasing the difference of $\delta^{13}C$ between different heights.

Stepwise regression analysis of ΔCO_2 and $\Delta\delta^{13}C$ and environmental factors during the growing season (Table 3) showed that during the day, ΔCO_2 and $\Delta\delta^{13}C$ responded mainly to the changes in Ta, showing very significant positive correlation ($P < 0.001$). Increase of Ta increased the activity of plant respiratory enzymes, stimulated the activity of soil microorganisms, promoted the C release of Ra and Rh, and depleted the ^{13}C of CO_2 in the atmosphere, resulting in a corresponding increase in $\Delta\delta^{13}C$. At night, after the Ta decreased, ΔCO_2 and $\Delta\delta^{13}C$ responded mainly to changes in RH, showing very significant negative correlation ($P < 0.001$). Increase of RH inhibited the C release of Ra and Rh, and reduced the ^{13}C depletion of CO_2 in the atmosphere, which in turn led to corresponding decrease in $\Delta\delta^{13}C$.

3.7. Separation of C release components in forests

Results showed that changes of CO_2 concentration occurred mainly at night and in the forest. The main pathway of C release in the *L. gmelinii* ecosystem was via Ra with a contribution rate of 51.18%, i.e., slightly higher

Table 3
Stepwise regression analysis of ΔCO_2, $\Delta\ \delta^{13}C$ and environmental factors in *Larix gmelinii* ecosystem.

Item	Time	Stepwise regression equation	Coefficient R^2	Significance P	Number n
ΔCO_2	Daytime 06:00–18:00	$\Delta CO_2 = 11.630\ Ta^{***} - 58.107\ VPD^{***} + 0.948\ RH^{*} - 169.720$	0.659	<0.001	4176
	Nighttime 18:00–06:00	$\Delta CO_2 = -0.796\ RH^{***} - 25.369\ WS^{*} + 122.730$	0.715	<0.001	4176
$\Delta\ \delta^{13}C$	Daytime 06:00–18:00	$\Delta\ \delta^{13}C = 0.399\ Ta^{***} - 1.707\ VPD^{***} + 0.045\ RH^{*} - 7.046$	0.809	<0.001	4176
	Nighttime 18:00–06:00	$\Delta\ \delta^{13}C = -0.055\ RH^{***} - 2.635\ WS^{*} + 6.515^{**}$	0.783	<0.001	4176

*** Means $P < 0.001$.
** Means $P < 0.01$.
* Means $P < 0.05$.

than the contribution rate of Rh (48.82%) (Fig. 7). The contribution rate of leaf respiratory C release of Ra was the highest, reaching 34.13%, followed by stems (33.53%) and roots (32.34%). For Rh, the contribution rate of C release during the decomposition process of litter was 51.78%, which was higher than the contribution of the decomposition of soil organic matter (48.22%), and indicated that the CO_2 released during the litter decomposition process was the main source for ecosystem CO_2 lake formation. Therefore, the contribution of litter decomposition to the C cycle of the ecosystem is very important and cannot be ignored.

4. Discussion

4.1. CO_2 concentration and its $\delta^{13}C$ dynamics

Ecosystem CO_2 concentration and its $\delta^{13}C$ stratification are extremely susceptible to the influence of atmospheric stability and exhibit complex spatial changes over short periods (Lee et al., 2007). During the day, the atmosphere is generally in an unstable state and thermal turbulence generates upward airflow, which drives the CO_2 at the bottom of the forest to flow toward the canopy. The leaves of the canopy absorb CO_2 during photosynthesis, which decreases the CO_2 concentration under the canopy and thus its concentration decreases with increase in vertical height (Broadmeadow et al., 1992). The CO_2 concentration above the canopy is higher than that at the canopy and lower than that below the canopy (Selm, 1952). As vertical height increases, turbulent mixing between the atmosphere of the forest and the background atmosphere intensifies, and the near-surface layer is affected more than the canopy by this atmospheric turbulent mixing. Therefore, the $\delta^{13}C$ below the canopy increases with vertical height (Takagi, 2009). At night, the atmosphere is mostly in a stable state, causing the CO_2 concentration of the ecosystem to decrease with increase of vertical height; however, the $\delta^{13}C$ shows an increasing variation (Flanagan et al., 2012). On a longer temporal scale, the CO_2 concentration of the ecosystem and its $\delta^{13}C$ show very significant negative correlation (Lai et al., 2005; Pataki et al., 2003). Schaeffer et al. (2008) studied the CO_2 concentration and its $\delta^{13}C$ changes in subalpine coniferous forests. They found that increase in atmospheric stability at night led to more obvious CO_2 concentration and its $\delta^{13}C$ stratification at different heights.

Studying the changes of CO_2 concentration and its $\delta^{13}C$ is an effective method to analyze the physiological and biochemical reactions during photosynthesis and respiration (Bowling et al., 2008; Scholze et al., 2003). In the process of photosynthesis and respiration, isotope $^{12}CO_2$ is preferentially absorbed or released, resulting in enrichment or depletion of ^{13}C in the atmosphere (Bowling et al., 2002). Buchmann et al. (1996b) found that C_3 and C_4 plants exhibited strongest photosynthetic C absorption at noon, causing lower canopy CO_2 concentration but with maximum $\delta^{13}C$ values.

Our results showed that at around 11:00, the CO_2 concentration in the middle layer of the canopy was 1.32 and 1.06 ppm lower than that in the upper and lower layers, respectively. (Fig. 4a). The $\delta^{13}C$ in the middle layer of the canopy was enriched by 0.83‰ and 0.64‰ in comparison with the upper and lower layers (Fig. 4b), respectively. The main reason for the abovementioned difference was that the intensity of photosynthetic C absorption by the canopy was relatively large. The maximum difference in C imbalance in the canopy at noon was generally <3‰ (Ogée et al., 2004). At night, affected by the temperature inversion layer, the CO_2 released from respiration accumulated in the forest and reached the diurnal

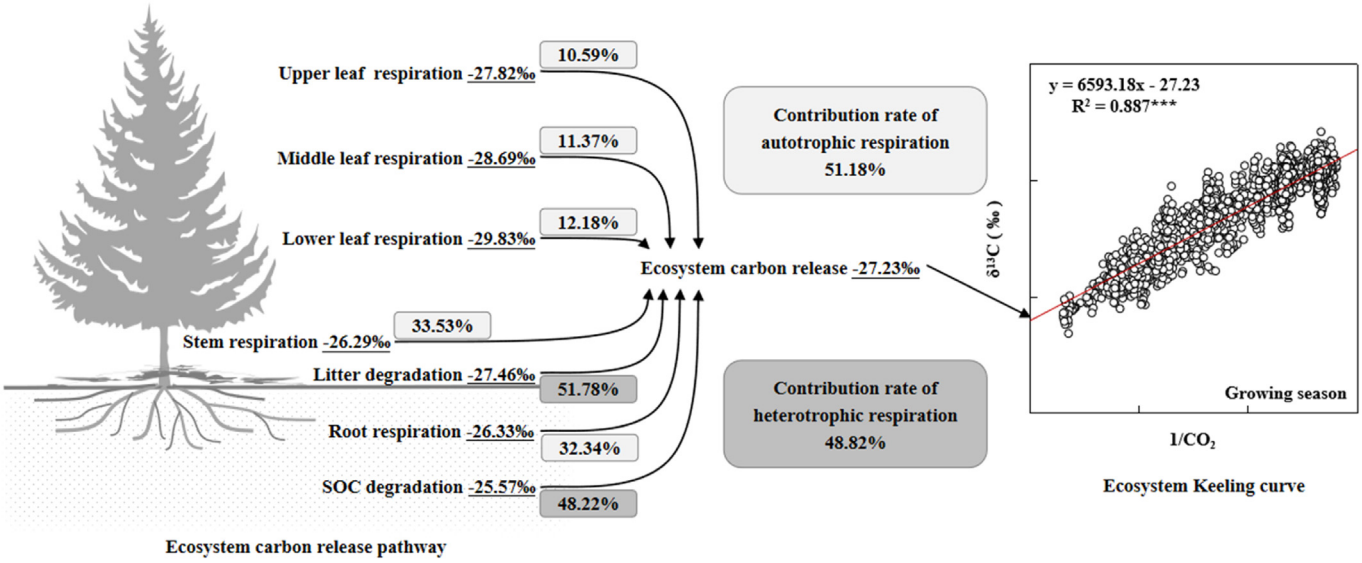

Fig. 7. Carbon release pathway and contribution rate of *Larix gmelinii* ecosystem. The underlined numbers are the carbon isotopic composition values of carbon release. The numbers with color blocks are the contribution rate of carbon release. The light and dark blocks represent the contribution rates of autotrophic and heterotrophic respiration, respectively. The red line represents Keeling Plot equation, and its intercept represents the carbon isotopic composition value of CO_2 released by the ecosystem.

peak before sunrise (Wu et al., 2005). The flux "flushing" phenomenon occurred after sunrise, and the CO_2 concentration dropped rapidly (Zhang et al., 2007). Respiratory C release from the canopy of *L. gmelinii* at night (18:00–06:00 next day) caused the CO_2 concentration in the lower canopy to be 17.07 and 6.09 ppm higher than that in the middle and upper layers (Fig. 4a), respectively. The $\delta^{13}C$ in the lower canopy was depleted by 0.68‰ and 0.29‰ in comparison with that in the middle and upper layers (Fig. 4b), respectively, which is a result similar to that of Zobitz et al. (2007) who found that the difference in C imbalance of a fir forest canopy was within ±2‰.

4.2. Source of CO_2 lakes

Chen et al. (2001) studied the temporal and spatial distributions of CO_2 concentration in tropical rainforests in Jianfengling, China. They found that the change of CO_2 concentration occurred mainly below the canopy, and that the CO_2 concentration in the near-surface layer was higher than that in the canopy. They also showed that the daily variation of CO_2 concentration was determined mainly by the accumulation of CO_2 concentration near the surface at night, and that the CO_2 concentration of the near-surface layer in the dry season was higher than that in the rainy season. Zhang et al. (2007) studied the temporal and spatial distributions of CO_2 concentration in tropical rainforests in Xishuangbanna, China. They reported that the near-surface CO_2 concentration was higher in the rainy season than that in the dry season. Our results showed that the concentration of CO_2 in the near-surface layer in the rainy season was higher than that in the less rainy season (Fig. 4a). The time of peak CO_2 concentration in the near-surface layer of different forests is very different, but the unifying feature is that when a CO_2 lake phenomenon occurs, it is often accompanied by the peak CO_2 concentration. This shows that the change of near-surface CO_2 concentration has considerable impact on the formation of CO_2 lakes. There are various types of CO_2 lake, including multimodal and unimodal (Zhang et al., 2007). On the daily scale, when the *L. gmelinii* ecosystem was a C source (17:00–06:00) (Li and Zhang, 2015), the phenomenon of a CO_2 lake often occurred. On the scale of the growing season, the strongest CO_2 lake was accompanied by the emergence of maximum respiratory flux (July–August) (Li, 2016). Therefore, the occurrence and intensity of a CO_2 lake is bound to affect the change of forest C flux, which affects the net C uptake of a forest (Zhang et al., 2007). It was found that the CO_2 lake effect has substantial impact on the C source/sink of the *L. gmelinii* ecosystem, and further research on this topic is required.

It was established that the main pathway of C release in the *L. gmelinii* ecosystem is via autotrophic respiration (Fig. 7), which is similar to the results of Zhu et al. (2013) who used eddy covariance technology to split the C release components of typical forest ecosystems in China, which were maintained at 51%. In our study, discrete sampling of the $\delta^{13}C$ in plants and soil had low time resolution. Incomplete capture was easy to occur in the process of CO_2 purification, which would lead to deviation in the determination results. When using linear model to split, the influence of these deviations on the split results could not be ignored, resulting in a certain degree of uncertainty in the split results. Therefore, in the future research, it is necessary to obtain respiration $\delta^{13}C$ values of different ecosystem components in a smaller time scale to reduce its uncertainty. The CO_2 released during litter decomposition was the main source for the formation of CO_2 lakes in this ecosystem. This phenomenon might be caused by the staggered distribution of the permafrost and island-like frozen soil within the study area, and the seasonal freeze–thaw phenomenon of the soil (Zhang et al., 2021). Frequent freeze–thaw alternation can change the physical and chemical properties and biological processes of the soil, leading to faster rate of decomposition litter, which can exceed the C fixation rate of microorganisms, resulting in net release of organic C (Gao et al., 2021). Global warming will affect litter decomposition through direct temperature effects and indirect changes in soil microorganisms (Aerts, 2006; Henry, 2007). Under the background of global climate change, the freeze–thaw pattern of the *L. gmelinii* ecosystem has changed substantially (Leng et al., 2008; Li et al., 2006), which will indirectly affect the primary productivity of the ecosystem. Therefore, the contribution of litter decomposition to the C cycle of the ecosystem is very important and cannot be ignored.

4.3. Drivers of CO_2 lakes

In addition to plant physiological activities, decomposition of residual organic matter, and atmospheric stability, SR, Ta, P, RH, and WS might all affect the CO_2 concentration and its $\delta^{13}C$ changes in the ecosystem (Barbour et al., 2011; Zobitz et al., 2007). The changes of CO_2 concentration and its $\delta^{13}C$ in the surface layer were controlled mainly by Ts5 (Table 2), while the CO_2 concentration and its $\delta^{13}C$ changes of the shrub layer and above were driven mainly by Ta (Li et al., 2017). Increase in Ts stimulates the activity of soil microorganisms, promotes the decomposition of litter and soil organic matter, and thus promotes soil respiration and CO_2 release (Li et al., 2020; Schipper et al., 2014). Increase in Ta affects the activity of plant respiratory enzymes, promotes plant respiration, and promotes plant respiration to release CO_2 (Crous et al., 2011; Teskey and Mcguire, 2010). In the context of global climate change, the rate of increase of temperature in the study area is 0.4 °C/decade (2011–2020) (Zhang et al., 2017), and the index regression analysis ($y = 431.71e^{0.0027x}$, $P < 0.001$, $R^2 = 0.836$) showed that the sensitivity of CO_2 concentration and its $\delta^{13}C$ to temperature (Q_{10}) was 1.0273. Under natural conditions, with temperature projected to continue to increase, the CO_2 concentration shows a significant upward trend (2020–2047) (Table 4) with a rate of CO_2 concentration increase of 17.22 ppm/decade. Thus, by 2047, the CO_2 concentration would be 1.17 times that of 2020. The $\delta^{13}C$ shows a significant trend of depletion with a depletion rate of 0.73‰/decade.

The CO_2 concentration and its $\delta^{13}C$ changes caused by the CO_2 lake phenomenon occurred mainly below the canopy (Zhang et al., 2007). On the half-hour time scale, the ΔCO_2 and $\Delta\delta^{13}C$ below the canopy during the day responded mainly to changes in Ta (Table 3). After Ta decreased at night, ΔCO_2 and $\Delta\delta^{13}C$ responded mainly to RH (Sun et al., 2015). Studies on subalpine coniferous forests have shown that ΔCO_2 and $\Delta\delta^{13}C$ have significant correlation with saturated VPD (Schaeffer et al., 2008), and VPD is calculated based on Ta and RH (Campbell and Norman, 1998). Therefore, on a short time scale, Ta and RH are important environmental factors that affect ΔCO_2 and $\Delta\delta^{13}C$ below the canopy of the *L. gmelinii* ecosystem.

4.4. Topography and formation of CO_2 lakes

A seasonal stagnant wetland is located to the south of the observation tower at a distance of 160 m (Fig. 8 left). Its average C release rate (190.47 $mg{\cdot}m^{-2}{\cdot}h^{-1}$) during the growing season was higher than that of *Ledum palustre–L. gmelinii* forests (172.41 $mg{\cdot}m^{-2}{\cdot}h^{-1}$) around the observation tower. A long-term flooded wetland is located to the east of the tower at a distance of 780 m. The average C release rate (131.16 $mg{\cdot}m^{-2}{\cdot}h^{-1}$) of the wetland in the growing season was slightly lower than that of the *Ledum palustre–L. gmelinii* forests (160.82 $mg{\cdot}m^{-2}{\cdot}h^{-1}$) (Chen, 2012). The soil C release variations of the three land types are all consistent with CO_2 lakes, and peaks occurred when both the Ta and the P reached their respective peaks (Fig. 8 right). The Chaocha River lies to the west of the observation tower at an average horizontal distance of 690 m. Studies have revealed obvious seasonal difference in the C release of the river, i.e., it is greatest in summer, lowest in winter, and that in autumn is greater than that in spring (Zhang et al., 2013). In addition to the effects of aquatic organisms, Ta and

Table 4
CO_2 concentration and its $\delta^{13}C$ with the trend of global climate change.

Year	2011	2020	2029	2038	2047
MAT (°C)	−5.8	−5.4	−5.0	−4.6	−4.2
CO_2 CONC (ppm)	402.17	419.39	436.61	453.83	471.05
$\delta^{13}C$ (‰)	−10.53	−11.26	−11.99	−12.72	−13.45

MAT and CONC represent the annual average temperature and gas concentration, respectively.

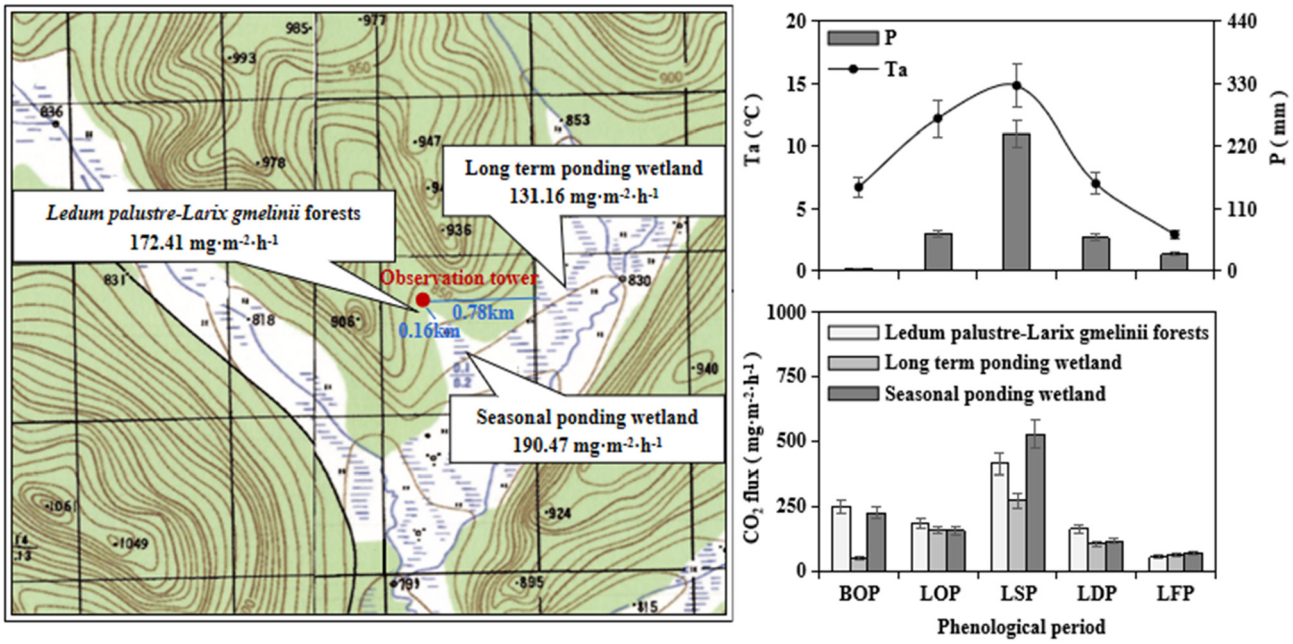

Fig. 8. The average rate of carbon release from different land types around the observation tower in growing season. The blue line and number represent the straight-line distance between the observation tower and the water area.

P also have certain impact on C release by the river (Wallin et al., 2020). To the north of the observation tower is a high mountain, the relative height difference between its bottom and the surrounding mountain top is 58–97 m, and the horizontal distance is 350–740 m. The general topography of the study area is funnel-shaped, and the mobility of air in the narrow area at the bottom is poor, causing CO_2 released from the forests, wetlands, and river to accumulate there, resulting in a CO_2 lake phenomenon.

5. Conclusions

(1) The CO_2 concentration and its $\delta^{13}C$ at different heights in the *L. gmelinii* ecosystem showed obvious stratification with a single-peak variation on the growing-season scale and the daily scale, which was closely related to plant metabolism and environmental factors.
(2) CO_2 lake phenomena occur in the forest areas in the northern part of the Greater Khingan Mountains. The intensity of CO_2 lakes was greater in the rainy season than in the less rainy season, greater at night than during the day, and greater in the early morning than in the evening. The appearance of a CO_2 lake and its strength responded mainly to temperature changes.
(3) The CO_2 concentration changes caused by the CO_2 lake phenomenon occurred mainly below the canopy, and the CO_2 concentration in the near-surface layer was higher than that in the canopy. When the *L. gmelinii* ecosystem was a C source, the CO_2 lake phenomenon often occurred. The strongest CO_2 lake was accompanied by the peak of ecosystem respiratory flux.
(4) The main pathway of C release in the *L. gmelinii* ecosystem is via Ra. The CO_2 released during litter decomposition was the main source of CO_2 lake formation, and the contribution of litter decomposition to the C cycle of the ecosystem was very important.
(5) In addition to the effects of environmental factors and litter decomposition, topography was also particularly important for the formation of CO_2 lakes. The overall funnel-shaped topography was conducive to the accumulation of CO_2 at the bottom of the study area and to the formation of a CO_2 lake.

CRediT authorship contribution statement

Xin Zhang: Conceptualization, Methodology, Formal analysis, Investigation, Data curation, Writing – original draft, Writing – review & editing. **Qiuliang Zhang:** Conceptualization, Methodology, Writing – original draft, Writing – review & editing, Funding acquisition, Supervision, Project administration. **Shoujia Sun:** Formal analysis, Investigation, Writing – original draft, Writing – review & editing. **Zhihong Xu:** Formal analysis, Writing – original draft, Writing – review & editing. **Yanan Jian:** Formal analysis, Writing – original draft, Writing – review & editing. **Yue Yang:** Formal analysis, Writing – original draft, Writing – review & editing. **Yuan Tian:** Formal analysis, Writing – original draft, Writing – review & editing. **Rula Sa:** Formal analysis, Writing – original draft, Writing – review & editing. **Bing Wang:** Formal analysis, Writing – original draft, Writing – review & editing. **Fei Wang:** Formal analysis, Writing – original draft, Writing – review & editing.

Declaration of competing interest

The authors declare that they have no known competing financial interests or personal relationships that could have appeared to influence the work reported in this paper.

Acknowledgments

We are grateful for the help and support of staff members at the National Field Scientific Observation and Research Station of Greater Khingan Forest Ecosystem, Inner Mongolia.

Funding information

This project was supported by the Regional Program of National Natural Science Foundation of China (grant no. 32060262) and the Training Program of National Natural Science Foundation of China (grant no. 2021GJYY003).

Availability of data and materials

The datasets generated and/or analyzed during the current study are not publicly available due [the data is a part of the author's graduation thesis] but are available from the corresponding author on reasonable request.

References

Aerts, R., 2006. The freezer defrosting: global warming and litter decomposition rates in cold biomes. J. Ecol. 94 (4), 713–724. https://doi.org/10.1111/j.1365-2745.2006.01142.x.

Atkin, O.K., Millar, H., Turnbull, M.H., 2010. Plant respiration in a changing world. New Phytol. 187, 268–272 https://www.jstor.org/stable/40792376 https://www.jstor.org/stable/40792376.

Barbour, M.M., Hunt, J.E., Kodama, N., Laubach, J., McSeveny, T.M., Rogers, G.N., Tcherkez, G., Wingate, L., 2011. Rapid changes in δ13C of ecosystem-respired CO2 after sunset are consistent with transient 13C enrichment of leaf respired CO2. New Phytol. 190, 990–1002. https://doi.org/10.1111/j.1469-8137.2010.03635.x.

Boone, R.D., Nadelhoffer, K.J., Canary, J.D., Kaye, J.P., 1998. Roots exert a strong influence on the temperature sensitivity of soil respiration. Nature 396, 570–572. https://doi.org/10.1038/25119.

Bowling, D.R., McDowell, N.G., Bond, B.J., Law, B.E., Ehleringer, J.R., 2002. 13C content of ecosystem respiration is linked to precipitation and vapor pressure deficit. Oecologia 131, 113–124. https://doi.org/10.1007/s00442-001-0851-y.

Bowling, D.R., Pataki, E.E., Randerson, J.T., 2008. Carbon isotopes in terrestrial ecosystem pools and CO2 fluxes. New Phytol. 178, 24–40. https://doi.org/10.1111/j.1469-8137.2007.02342.x.

Broadmeadow, M., Griffiths, H., Maxwell, C., Borland, A., 1992. The carbon isotope ratio of plant organic material reflects temporal and spatial variations in CO2 within tropical forest formations in Trinidad. Oecologia 89, 435–441. https://doi.org/10.1007/BF00317423.

Buchmann, N., 2002. Plant ecophysiology and forest response to global change. Tree Physiol. 22, 1177–1184. https://doi.org/10.1093/treephys/22.15-16.1177.

Buchmann, N., Kao, W.Y., Ehleringer, J.R., 1996b. Carbon dioxide concentrations within forest canopies: variation with time, stand structure, and vegetation type. Glob. Chang. Biol. 2 (5), 421–432. https://doi.org/10.1111/j.1365-2486.1996.tb00092.x.

Buchmann, N.R., Brooks, K.D., Ehleringer, J.R., 1996a. Carbon isotope composition of C4 grasses is influenced by light and water supply. Plant Cell Environ. 19, 392–402. https://doi.org/10.1111/j.1365-3040.1996.tb00331.x.

Buchmann, N., Kao, W.Y., Ehleringer, J.R., 1997. Influence of stand structure on carbon-13 of vegetation, soils, and canopy air within deciduous and evergreen forests in Utah, United States. Oecologia 110, 109–119. https://doi.org/10.1007/s004420050139.

Cai, T.B., Flanagan, L.B., Jassal, R.S., Black, T.A., 2008. Modelling environmental controls on ecosystem photosynthesis and the carbon isotope composition of ecosystem-respired CO2 in a coastal Douglas-fifir forest. Plant Cell Environ. 31, 435–453. https://doi.org/10.1111/j.1365-3040.2008.01773.x.

Campbell, G.S., Norman, J.M., 1998. An Introduction to Environmental Biophysics. Springer-verlag, New York, Heidelberg, pp. 41–42.

Chen, G.W., 2012. Study soil GHG fluxes of Lartix gmelinii forest. (PhD Dissertation)Inner Mongolia Agricultural University. https://kns.cnki.net.

Chen, B.Z., Chen, J.M., 2007. Diurnal, seasonal and interannual variability of carbon isotope discrimination at the canopy level in response to environmental factors in a boreal forest ecosystem. Plant Cell Environ. 30, 1223–1239. https://doi.org/10.1111/j.1365-3040.2007.01703.x.

Chen, B.F., Lin, M.X., Li, Y.D., Qiu, J.R., Luo, T.S., Zhou, T.F., 2001. Space-time character of CO2 content in tropical mountain rain forest of Jianfengling,Hainan. Acta Ecol. Sin. 21 (12), 2089–2095 https://kns.cnki.net https://kns.cnki.net.

CMA Climate Change Centre, 2021. Blue Book on Climate Change in China (2021). Science Press, Beijing, pp. 3–5 (In Chinese).

Crous, K.Y., Zaragoza-Castells, J., Low, M., Ellsworth, D.S., Tissue, D.T., Tjoelker, M.G., Barton, C.M., Gimeno, T.E., Atkin, O.K., 2011. Seasonal acclimation of leaf respiration in Eucalyptus saligna trees: impacts of elevated atmospheric CO2 and summer drought. Glob. Chang. Biol. 17 (4), 1560–1576. https://doi.org/10.1111/j.1365-2486.2010.02325.x.

Davidson, E.A., Janssens, I.A., Luo, Y.Q., 2006. On the variability of respiration in terrestrial ecosystems: moving beyond Q10. Glob. Chang. Biol. 12 (2), 154–164. https://doi.org/10.1111/j.1365-2486.2005.01065.x.

Dawson, T.E., Mambelli, S.H., Plamboeck, A.H., Templer, P.H., Kevin, P.T., 2002. Stable isotope in plant ecology. Annu. Rev. Ecol. Syst. 33, 507–559. https://doi.org/10.1146/annurev.ecolsys.33.020602.095451.

Duursma, R.A., Barton, C.M., Lin, Y.S., Medlyn, B.E., Eamus, D., Tissue, D.T., Ellsworth, D.S., McMurtrie, R.E., 2014. The peaked response of transpiration rate to vapour pressure deficit in field conditions can be explained by the temperature optimum of photosynthesis. Agric. For. Meteorol. 189, 2–10. https://doi.org/10.1016/j.agrformet.2013.12.007.

Fan, S.M., Wofsy, S.C., Bakwin, P.S., Jacob, D.J., Fitzjarrald, D.R., 1990. Atmosphere-biosphere exchange of CO2 and O3 in the central Amazon Forest. J. Geophys. Res. Atmos. 95 (10), 16851–16864. https://doi.org/10.1029/JD095iD10p16851.

Farquhar, G.D., Ehleringer, J.R., Hubick, K.T., 1989. Carbon isotope discrimination and photosynthesis. Annu. Rev. Plant Physiol. Plant Mol. Biol. 40, 503–537. https://doi.org/10.1146/annurev. pp. 40.060189.002443.

Fassbinder, J.J., Griffis, T.J., Baker, J.M., 2012. Evaluation of carbon isotope flux partitioning theory under simplified and controlled environmental conditions. Agric. For. Meteorol. 153, 154–164. https://doi.org/10.1016/j.agrformet.2011.09.020.

Flanagan, L.B., Ehleringer, J.R., Pataki, D.E., 2005. Stable Isotopes And Biosphere: Atmosphere Interactions. Academic Press, Netherlands, pp. 125–153 https://doi.org/10.1016/B978-0-12-088447-6.X5000-4.

Flanagan, L., Cai, T., Black, T.A., Barr, A.G., McCaughey, J.H., Margolis, H.A., 2012. Measuring and modeling ecosystem photosynthesis and the carbon isotope composition of ecosystem-respired CO2 in three boreal coniferous forests. Agric. For. Meteorol. 153, 165–176. https://doi.org/10.1016/j.agrformet.2011.03.001.

Forkel, M., Carvalhais, N., Rödenbeck, C., Keeling, R., Heimann, M., Thonicke, K., Zaehle, S., Reichstein, M., 2016. Enhanced seasonal CO2 exchange caused by amplified plant productivity in northern ecosystems. Science 351 (6274), 696–699. https://doi.org/10.1126/science.aac4971.

Gao, J., Wei, X.Y., Chen, Y., Dong, Y.L., Yang, Y.L., Zhnag, D.J., 2021. Litter decomposition rates and organic carbon dynamics in subalpine forest during freeze-thaw cycles. Acta Ecol.Sin.(In Chinese). 41 (9), 3734–3743 https://kns.cnki.net https://kns.cnki.net.

Grace, J., Rayment, M., 2000. Respiration in the balance. Nature 404, 859–860. https://doi.org/10.1038/35009170.

Griffis, T.G., 2013. Tracing the flow of carbon dioxide and water vapor between the biosphere and atmosphere: a review of optical isotope techniques and their application. Agric. For. Meteorol. 174–175, 85–109. https://doi.org/10.1016/j.agrformet.2013.02.009.

Griffith, D.T.W., Deutscher, N.M., Caldow, C., Kettlewell, G., Riggenbach, M., Hammer, S., 2012. A Fourier transform infrared trace gas and isotope analyzer for atmospheric applications. Atmos. Meas. Tech. 5, 2481–2498. https://doi.org/10.5194/amt-5-2481-2012.

Han, L., Wang, Q.F., Chen, Z., Yu, G.R., Zhou, S.G., Chen, S.P., Li, Y.N., Zhang, Y.P., Yan, J.H., Wang, H.M., Han, S.J., Wang, Y.F., Sha, L.Q., Shi, P.L., Zhang, Y.J., Xiang, W.H., Zhao, L., Zhang, Q.L., He, X.G., Guo, J.X., 2020. Spatial patterns and climate controls of seasonal variations in carbon fluxes in China's terrestrial ecosystems. Glob. Chang. Biol. 189. https://doi.org/10.1016/j.gloplacha.2020.103175.

Harris, N.L., Gibbs, D.A., Baccini, A., Birdsey, R.A., Bruin, S., Farina, M., Fatoyinbo, L., Hansen, M.C., Herold, M., Houghton, R.A., Potapov, P.V., Suarez, D.R., Roman-Cuesta, R.M., Saatchi, S.S., Slay, C.M., Turubanova, S.A., Tyukavina, A., 2021. Global maps of twenty-first century forest carbon fluxes. Nat. Clim. Chang. 11, 234–240. https://doi.org/10.1038/s41558-020-00976-6.

Henry, H.A.L., 2007. Soil freeze-thaw cycle experiments: trends, methodological weaknesses and suggested improvements. Soil Biol. Biochem. 39 (5), 977–986. https://doi.org/10.1016/j.soilbio.2006.11.017.

IPCC, 2007. Climate Change 2007: The Physical Science Basis. Cambridge University Press, UK, pp. 6–18 https://www.ipcc.ch.

IPCC, 2021. Climate Change 2021: The Physical Science Basis. Cambridge University Press, UK, pp. 5–15 https://www.ipcc.ch.

Jiang, Y.L., Zhou, G.S., 2001. Carbon balance and global change of Larix gmeliniii forest. Chin. J. Appl. Ecol. 12 (4), 481–484 (In Chinese) https://kns.cnki.net.

Keeling, C.D., 1958. The concentration and isotopic abundances of atmospheric carbon dioxide in rural areas. Geochim. Cosmochim. Acta 13, 322–334. https://doi.org/10.1016/0016-7037(58)90033-4.

Klumpp, K., Schaufele, M., Lotscher, M., Lattanzi, F.A., Feneis, W., Schnyder, H., 2005. C-isotope composition of CO2 respired by shoots and roots: fractionation during dark respiration? Plant Cell Environ. 28, 241–250. https://doi.org/10.1111/j.1365-3040.2004.01268.x.

Lai, C.T., Ehleringer, J.R., Schauer, A.J., Tans, P.P., Hollinger, D.Y., Paw, K.T., Munger, J.W., Wofsy, S.C., 2005. Canopy-scale δ13C of photosynthetic and respiratory CO2 fluxes: observations in forest biomes across the United States. Glob. Chang. Biol. 11 (4), 633–643. https://doi.org/10.1111/j.1365-2486.2005.00931.x.

Lee, X.H., Kim, K., Smith, R., 2007. Temporal variations of the 18O/16O signal of the whole-canopy transpiration in a temperate forest. Glob. Biogeochem. Cycles 21, 1–12. https://doi.org/10.1029/2006GB002871.

Leng, W.F., He, H.S., Liu, H.J., 2008. Response of larch species to climate changes. J. Plant Ecol. 1, 203–205. https://doi.org/10.1093/jpe/rtn013.

Li, X.M., 2016. Study on carbon flux and its characteristics and influencing factors in Larix Gmelinii forest ecosystem. (PhD Dissertation)Inner Mongolia Agricultural University. https://kns.cnki.net.

Li, X.M., Zhang, Q.L., 2015. Impact of climate factors on CO2 flux characteristics in a Larix gmelinii forest ecosystem. J. Beijing For. Univ. 37, 31–39 https://kns.cnki.net https://kns.cnki.net.

Li, F., Zhou, G.S., Cao, M.C., 2006. Simulation of geographical distribution response of Larix gmeliniii to climate change. Chin. J. Appl. Ecol. 17, 2255–2260 https://kns.cnki.net https://kns.cnki.net.

Li, H.Z., Yu, X.X., Jia, G.D., Zhao, N., Liu, Z.Q., Lu, W.W., Zhang, Y.E., 2017. Variations and determinants of CO2 concentration and δ13C in Platycladus orientalis plantation in Beijing mountainous area,China. Chin. J. Appl. Ecol. 28 (7), 2164–2170 https://kns.cnki.net https://kns.cnki.net.

Li, J.Q., Pei, J.M., Pendall, E., Fang, C.M., Nie, M., 2020. Spatial heterogeneity of temperature sensitivity of soil respiration: a global analysis of field observations. Soil Biol. Biochem. 141, 107675. https://doi.org/10.1016/j.soilbio.2019.107675.

Lin, G.H., 2013. Stable Isotope Ecology. Higher Education Press, Beijing, pp. 102–105 (In Chinese).

Lin, G.H., Ehleringer, J.R., 1997. Carbon isotopic fractionation does not occur during dark respiration in C3 and C4 plants. Plant Physiol. 114 (1), 391–394. https://doi.org/10.1104/pp.114.1.391.

Lloyd, J., Taylor, J.A., 1994. On the temperature dependence of soil respiration. Funct. Ecol. 8, 315–323. https://doi.org/10.2307/2389824.

McNaughton, S.J., Oesterheld, M., Frank, D.A., Williams, K.J., 1989. Ecosystem-level patterns of primary productivity and herbivory in terrestrial habitats. Nature 341, 142–144. https://doi.org/10.1038/341142a0.

Mohanal, M., Siddiquial, T.A., 1998. Analysis of various schemes for the estimation of atmospheric stability classification. Atmos. Environ. 32 (21), 3775–3781. https://doi.org/10.1016/S1352-2310(98)00109-5.

Moyes, A.B., Gaines, S.J., Siegwolf, R.W., Bowling, D.R., 2010. Diffusive fractionation complicates isotopic partitioning of autotrophic and heterotrophic sources of soil respiration. Plant Cell Environ. 33, 1804–1819. https://doi.org/10.1111/j.1365-3040.2010.02185.x.

Ogée, J., Peylin, P., Ciais, P., Bariac, T., Brunet, Y., Berbigier, P., Bonnefond, J.M., 2003. Partitioning net ecosystem carbon exchange into net assimilation and respiration using 13CO2 measurements: a cost effective sampling strategy. Glob. Biogeochem. Cycles 17 (2). https://doi.org/10.1029/2002GB001995.

Ogée, J., Peylin, P., Cunta, M., Bariac, T., Brunet, Y., Berbigier, P., Richard, P., Ciais, P., 2004. Partitioning net ecosystem carbon exchange into net assimilation and respiration with canopy-scale isotopic measurements: an error propagation analysis with 13CO2 and CO18 O data. Glob. Biogeochem. Cycles 18 (2). https://doi.org/10.1029/2003GB002166.

Pataki, D., Bowling, D., Eheleringer, J., 2003. Seasonal cycle of carbon dioxide and its isotope dioxide and its isotope composition in an urban atmosphere: anthropogenic and biogenic effects. J. Geophys. Res. Atmos. 108 (23), 4375. https://doi.org/10.1029/2003JD003865.

Schaeffer, S.M., Anderson, D.E., Burns, S.P., Monson, R.K., Sun, J.L., Bowing, D.R., 2008. Canopy structure and atmospheric flows in relation to the δ13C of respired CO2 in a subalpine coniferous forest. Agric. For. Meteorol. 148 (4), 592–605. https://doi.org/10.1016/j.agrformet.2007.11.003.

Schipper, L.A., Hobbs, J.K., Rutledge, S., Arcus, V.L., 2014. Thermodynamic theory explains the temperature optima of soil microbial processes and high Q10 values at low temperatures. Glob. Chang. Biol. 20, 3578–3586. https://doi.org/10.1111/gcb.12596.

Scholze, M., Kaplan, J.O., Knorr, W., Heimann, M., 2003. Climate and interannual variability of the atmosphere-biosphere 13CO2 flux. Geophys. Res. Lett. 30 (2), 67. https://doi.org/10.1029/2002GL015631.

Selm, H.R.D., 1952. Carbon dioxide gradient in a beech forest in central Ohio. Ohio J. Sci. 52 (4), 187 https://kb.osu.edu/bitstream/handle/1811/3939/1/V52N04_187 https://kb.osu.edu/bitstream/handle/1811/3939/1/V52N04_187.

Sun, S.J., Meng, P., Zhang, J.S., Shu, J.H., Zheng, N., 2015. Differences and sources of CO2 concentration, carbon and oxygen stable isotope composition between inside and outside of a green space system and influencing factors in an urban area. Chin. J. Appl. Ecol. 26 (10), 3000–3010 https://kns.cnki.net https://kns.cnki.net.

Takagi, M., 2009. Atmospheric carbon dioxide concentration within a narrow valley in a forested catchment area. J. For. Res. 14 (5), 286–295. https://doi.org/10.1007/s10310-009-0138-4.

Teskey, R.O., Mcguire, M.A., 2010. Carbon dioxide transport in xylem causes errors in estimation of rates of respiration in stems and branches of trees. Plant Cell Environ. 25 (11), 1571–1577. https://doi.org/10.1046/j.1365-3040.2002.00961.x.

Tian, Y., Zhang, Q.L., Liu, X., Meng, M., 2018. Stem radius variation in response to hydrothermal factors in Larch. Forests 9, 602. https://doi.org/10.3390/f9100602.

Trumbore, S., 2006. Carbon respired by terrestrial ecosystems-recent progress and challenges. Glob. Chang. Biol. 12 (2), 141–153. https://doi.org/10.1111/j.1365-2486.2006.01067.x.

Wallin, M.B., Audet, J., Peacock, M., Sahlee, E., Winterdahl, M., 2020. Carbon dioxide dynamics in an agricultural headwater stream driven by hydrology and primary production. Biogeosciences 17 (9), 2487–2498. https://doi.org/10.5194/bg-17-2487-2020.

Wang, J., Feng, L., Palmer, P.L., Liu, Y., Fang, S.X., Bosch, H., O'Dell, C.W., Tang, X.P., Yang, D.X., Liu, L.X., Xia, C.Z., 2020. Large Chinese land carbon sink estimated from atmospheric carbon dioxide data. Nature 586, 720–723. https://doi.org/10.1038/s41586-020-2986-1.

Whiteman, C.D., Zhong, S., Shaw, W.J., Hubbe, J.M., Bian, X., Mittelstadt, J., 2001. Pools in the Columbia Basin. Weather Forecast. 16, 432–447. https://doi.org/10.1175/1520-0434(2001)016%3C0432:CPITCB%3E2.0.CO;2.

Wingate, L., Ogée, J., Burlett, R., Bosc, A., Devaux, M., Grace, J., Loustau, D., Gessler, A., 2010. Photosynthetic carbon isotope discrimination and its relationship to the carbon isotope signals of stem, soil and ecosystem respiration. New Phytol. 188 (2), 576–589. https://doi.org/10.1111/j.1469-8137.2010.03384.x.

Wu, J.B., Guan, X.D., Zhao, X.S., Han, S.J., Yu, D.R., Sun, X.M., 2005. CO2 concentration character in broad-leaved Korean pine forest of Changbai Mountains. J. Appl. Ecol. 16 (1), 49–53 ttps://kns.cnki.net https://kns.cnki.net.

Yakir, D., Sternberg, L.S., 2000. The use of stable isotopes to study ecosystem gas exchange. Oecologia 123, 297–311. https://doi.org/10.1007/s004420051016.

Yakir, D., Wang, X.F., 1996. Fluxes of CO2 and water between terrestrial vegetation and the atmosphere estimated from measurements. Nature 380, 515–517. https://doi.org/10.1038/380515a0.

Zhang, Y.P., Liang, N.S., Yao, Y.G., Tan, Z.H., Sha, L.Q., Gao, J.M., Song, Q.H., Zhang, M.D., Li, Z.H., Yang, Z., 2007. Characteristics and effects of carbon lake in the tropical mountainous region of Xishuangbanna, SW China. Proceedings of the conference of China Meteorological Society, pp. 434–457 (In Chinese).

Zhang, L.J., Wang, L., Cai, W.J., Liu, D.M., Yu, Z.G., 2013. Impact of human activities on organic carbon transport in the Yellow River. Biogeosciences 10 (4), 2513–2524. https://doi.org/10.5194/bg-10-2513-2013.

Zhang, Q.L., Bian, Y.M., Dai, H.Y., Wang, B., Feng, L.H., Wang, M.Y., 2017. Variation of extreme temperature events in Daxing'anling forest region of Inner Mongolia. Sci. Geogr. Sin. 37 (12), 1909–1916 https://kns.cnki.net https://kns.cnki.net.

Zhang, X., Zhang, Q.L., Xu, Z.H., Wang, R., Jian, Y.N., Yang, J.F., Sun, C.L., Wang, J.F., 2021. Mechanism of environmental factors regulating water consumption of Larix gmeliniii forests. J. Soils Sediments https://doi.org/10.1007/s11368-021-03025-7.

Zhu, X.J., Yu, G.R., Wang, Q.F., Gao, Y.N., Zhao, X.Q., Han, S.J., Yan, J.H., 2013. The interaction between components of ecosystem respiration in typical forest and grassland ecosystems. Acta Ecol. Sin. 33 (21), 6925–6934 https://kns.cnki.net https://kns.cnki.net.

Zobitz, J.M., Burns, S.P., Ogée, J., Reichstein, M., Bowling, D.R., 2007. Partitioning net ecosystem exchange of CO2: a comparison of a Bayesian/isotope approach to environmental regression methods. J. Geophys. Res. Biogeosci. 112 (G3). https://doi.org/10.1029/2006JG000282.